Human epidermal growth factor receptor 2 immunohistochemical analysis

Breast adenocarcinoma, analyzed as a positive control, showed strong immunoreactivity in the cell membrane (Fig. 1a).

In the normal kidney tissue specimens 6 of 12 cases with Wilms tumor were strongly positive (3+) and the other six cases were weakly positive (2+). HER2 showed a strong immunoreactivity in the cell membranes of the collecting tubules and endothelial cells, and weak staining in the proximal and distal convoluted tubules, whereas the glomeruli were not entirely stained (Fig. 1b).

In the Wilms tumors, the immunostaining for HER2 was diffuse and the findings tended to vary widely. Among the 15 specimens with epithelial cells, eight (53.3%) showed HER2 immunoreactivity mainly in the tumor cell membranes (Fig. 1c). Four of them showed strong immunoreactivity (3+), while the others showed weak to moderate immunoreactivity (2+). HER2 immunoreactive blastemal cells were present in 11 (45.8%) of 24 cases with blastemal cells mainly in the membranes and, to a minor extent, in the cytoplasm (Fig. 1d). All 11 cases showed weak to moderate immunoreactivity (2+). Only 3 (14.3%) of 21 specimens containing mesenchymal cells showed weak to moderate immunoreactivity (2+) in the cytoplasm (Fig. 1e).

Association between Her2 expression and prognosis

Among the 24 cases, two cases demonstrated recurrence while three cases died. All five cases showed a negative HER2 expression, except for one (case 20) who showed a weak HER2 expression, and all cases were also blastemal predominant.

Discussion

In the last decade there has been great interest in the HER2 proto-oncogene concerning tumor biology. A number of immunohistochemical studies have examined the clinicopathological significance of HER2 expression in cancers of various organs. An overexpression of the HER2 gene has been found to correlate with a poor prognosis in a variety of malignant tumors, such as breast, ovarian, and lung cancer [15]. In some

Table 2 Clinical, pathologic, and genetic characteristics of study specimens

Case	Histological phase	Predominant cell	HER2 expression			Prognosis
			Epithelial	Blastemal	Mesenchymal	
1	Triphasic	Epithelial	3+	2+	2+	Alive
2	Triphasic	Epithelial	3+	2+	1+	Alive
3	Triphasic	Epithelial	2+	1+	1+	Alive
4	Triphasic	Epithelial	1+	1+	1+	Alive
5	Triphasic	Blastemal	3+	1+	1+	Alive
6	Triphasic	Blastemal	2+	2+	1+	Alive
7	Triphasic	Blastemal	1+	2+	1+	Alive
8	Triphasic	Blastemal	1+	1+	2+	Alive
9	Triphasic	Blastemal	1+	1+	1+	REC
10	Triphasic	Blastemal	1+	1+	1+	Alive
11	Triphasic	Blastemal	1+	0	1+	Alive
12	Triphasic	Blastemal	1+	0	1+	DOD
13	Biphasic	Epithelial	2+	2+	NO	Alive
14	Biphasic	Blastemal	3+	2+	NO	Alive
15	Biphasic	Blastemal	2+	1+	NO	Alive
16	Biphasic	Blastemal	NO	2+	2+	Alive
17	Biphasic	Blastemal	NO	2+	1+	Alive
18	Biphasic	Blastemal	NO	2+	1+	Alive
19	Biphasic	Blastemal	NO	2+	1+	Alive
20	Biphasic	Blastemal	NO	2+	0	DOD
21	Biphasic	Blastemal	NO	1+	1+	Alive
22	Biphasic	Blastemal	NO	1+	1+	DOD
23	Biphasic	Blastemal	NO	0	0	REC
24	Biphasic	Blastemal	NO	0	0	Alive

DOD dead of disease, *NO* no corresponding cell present, *REC* recurrence

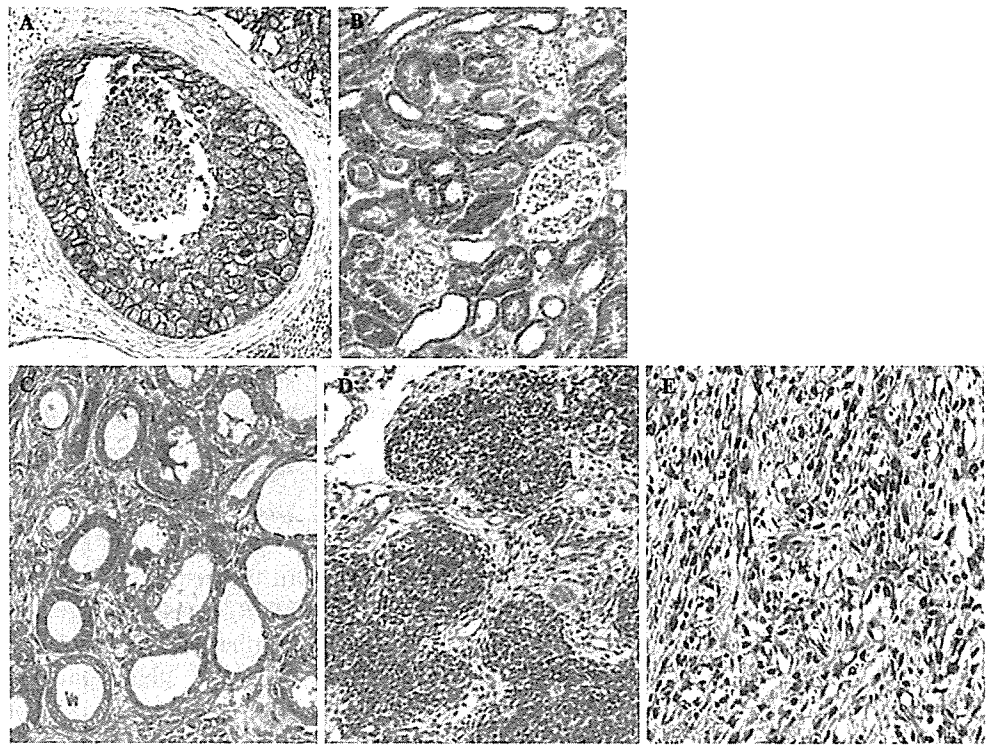

Fig. 1 Immunohistochemical staining for HER2 expression: **a** breast adenocarcinoma as a positive control shows strong positivity (3+); **b** normal kidney tissues specimens show strong positivity for the renal tubules (3+); **c** epithelial cell component showed strong positivity in renal tubule-like structures (3+); **d** blastemal cell component showed weak to moderate positivity (2+); **e** mesenchymal cell component showed weak to moderate positivity (2+)

of these tumors, an enhanced expression of HER2 has been reported to be associated with both an increased carcinogenicity and metastatic potential [12] or with resistance to chemotherapeutic agents [16, 17].

In Wilms tumors, the expression of HER2 has been analyzed in few reports. Ghanem et al. concluded that HER2 may not play an important role in the aggressive behavior of Wilms tumor [2]. Yokoi et al. suggested that erbB-2 in an in vivo model might serve as a therapeutic target [18, 19]. However, there is still a lack of general consensus regarding the possible prognostic impact of this marker in Wilms tumors, and it is still not clear whether HER2 may act jointly with other clinicopathological parameters to influence either the response to chemotherapy or the clinical outcome.

In the current study, we found HER2 protein to be expressed in all renal tubular structures, thus suggesting that HER2 protein is a normal membrane constituent of normal epithelial renal tissue. Interestingly, the staining patterns appear to differ regarding each component. The HER2 protein expression in immunoreactive epithelial cells was 53.3% and was 45.8% in blastemal cells, whereas the mesenchymal component stained only 14.3% (Fig. 2). Similar findings have also been confirmed in uterine carcinosarcoma [20–22] and biphasic synovial sarcoma [23], in which the HER2 expression was high in the epithelial component, while it was very low in the mesenchymal component (Fig. 2).

Some studies have revealed the HER2 overexpression to be associated with histological differentiation and a favorable prognosis in both thyroid carcinoma and synovial sarcoma [24–26]. In the present study, we assessed the association between the HER2 expression and prognosis in Wilms tumor. An HER2 overexpression might therefore be associated with a good prognosis in Wilms tumor; however, it is difficult to conclude due to the small number of cases under study.

Human epidermal growth factor receptor 2 proto-oncogene is located at 17q21 and it encodes a 185-kDa transmembrane tyrosine kinase glycoprotein with an extensive homology to the epidermal growth factor receptor (EGFR) [27, 28]. The presence of epidermal growth factor (EGF) peptides and their respective receptors has been found in normal developing kidney of mammalian embryos [29, 30]. In addition, EGF is required for kidney tubulogenesis in an ammonium sulfate-treated matrigel culture in a dose -dependent manner; a significantly higher dosage was required to stimulate the branching of tubules [31]. Wilms tumor is classified as a primitive, multilineage malignancy of embryonic renal precursors. Furthermore, it shares histological features with the developing normal kidney, and is frequently cited as an example of impaired differentiation in tumorigenesis [32]. Wilms tumor has been traditionally viewed as a triphasic embryonal tumor with epithelial, blastemal and mesenchymal components. The blastemal and epithelial components

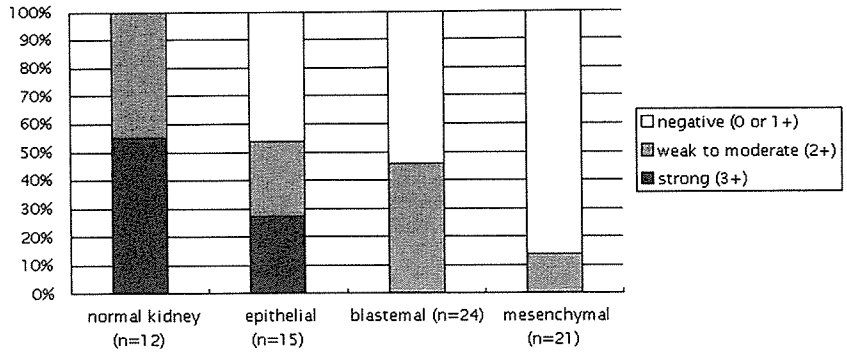

Fig. 2 HER2 score according to cell type: all normal kidney tissue specimens showed moderate to strong positivity (100%); epithelial component showed moderate (26.7%) to strong (26.7%) positivity; blastemal component showed weak to moderate (45.8%) positivity; mesenchymal component showed weak to moderate (14.3%) positivity

usually resemble structures seen during normal nephrogenesis, while the mesenchymal component may undergo heterogeneous differentiation [33].

In this study, we analyzed HER2 expression in different histological components of Wilms tumor, and showed that these components apparently have different levels of HER2 protein expression. According to these findings, we hypothesize the existence of the developmental pathway to be as follows (Fig. 3): the expression of HER2 is essential for differentiation to the normal kidney tissue (tubular formation, branching, and epithelial differentiation) during normal nephrogenesis. In the development of Wilms tumor, a high level of HER2 expression contributes to the generation of epithelial component; however, unknown growth factors may be associated with the generation of a mesenchymal and blastemal component.

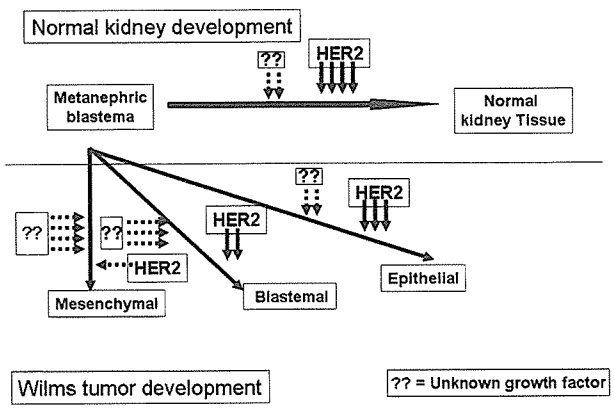

Fig. 3 Normal kidney and Wilms tumor development: during normal nephrogenesis, HER2 is essential for differentiating metanephric blastema to normal kidney tissue; in the development of Wilms tumor, a high level of HER2 expression contributes to the generation of an epithelial component; however, unknown growth factors may also be associated with the generation of a mesenchymal and blastemal component

In conclusion, the extent of the HER2 expression is thus considered to be associated with epithelial differentiation in Wilms tumor. These histological findings may therefore help to explain the development of Wilms tumor from the standpoint of histological differentiation.

Acknowledgments The authors thank Mr. Brian Quinn for reading the manuscript. This work was supported in part by the Grant-in-Aid for Scientific Research from the Japanese Society for the Promotion of Science.

References

1. Beckwith JB (1994) Renal neoplasm of childhood. In: Sternberg SS (eds) Diagnostic surgical pathology. Raven Press, New York, pp1741–1766
2. Ghanem MA, Van Der Kwast TH, Den Hollander JC, et al (2001) Expression and prognostic value of epidermal growth factor receptor, transforming growth factor-alpha, and c-erb B-2 in nephroblastoma. Cancer 92:3120–3129
3. Coussens L, Yang-Feng TL, Liao YC et al (1985) Tyrosine kinase receptor with extensive homology to EGF receptor shares chromosomal location with neu oncogene. Science 230:1132–1139
4. Slamon DJ, Godolphin W, Jones LA et al (1989) Studies of the HER-2/neu proto-oncogene in human breast and ovarian cancer. Science 244:707–712
5. Onda M, Matsuda S, Higaki S et al (1996) ErbB-2 expression is correlated with poor prognosis for patients with osteosarcoma. Cancer 77:71–78
6. Bargmann CI, Weinberg RA (1988) Increased tyrosine kinase activity associated with the protein encoded by the activated neu oncogene. Proc Natl Acad Sci USA 85:5394–5398
7. Shih C, Padhy LC, Murray M, et al (1981) Transforming genes of carcinomas and neruoblastomas introduced into mouse fibroblasts. Nature 290:261–264
8. Menard S (1999) HER2 overexpression in various tumor types. In: Proceedings of the HER2 state-of-the-art conference, Montreux, Switzerland
9. Liu E, Thor A, He M, et al (1992) The HER2 (c-erbB-2) oncogene is frequently amplified in insitu carcinomas of the breast. Oncogene 7:1027–1032
10. Lohrisch C, Piccart M (2001) An overview of HER2. Semin Oncol 28:3–11

11. van de Vijver MJ (2001) Assessment of the need and appropriate method for testing for the human epidermal growth factor receptor-2 (HER2). Eur J Cancer 37:11–17
12. Yu D, Wolf JK, Scanlon M, et al (1993) Enhanced c-erbB-2/neu expression in human ovarian cancer cells correlates with more severe malignancy than can be suppressed by E1A. Cancer Res 53:891–898
13. Woodburn JR (1999) The epidermal growth factor receptor and its inhibition in cancer therapy. Pharmacol Ther 82:241–250
14. Sakurai H, Tsukamoto T, Kjellsberg CA, et al (1997) EGF receptor ligands are a large fraction of in vitro branching morphogenesis secreted by embryonic kidney. Am J Physiol Renal Physiol 273:463–472
15. Hynes NE, Stern DF (1994) The biology of erbB-2/neu/HER-2 and its role in cancer. Biochim Biophys Acta 1198:165–184
16. Tsai CM, Yu D, Chang KT, et al (1995) Enhanced chemoresistance by elevation of p185neu levels in HER-2/neu-transfected human lung cancer cells. J Natl Cancer Inst 87:682–684
17. Yu D, Liu B, Tan M, et al (1996) Overexpression of c-erbB-2/neu in breast cancer cells confers increased resistance to taxol via mdr-1-independent mechanisms. Oncogene 13:1359–1365
18. Yokoi A, McCrudden KW, Huang J, et al (2003) Blockade of her2/neu decreases VEGF expression but does not alter HIF-1 distribution in experimental Wilms tumor. Oncol Rep 10:1271–1274
19. Yokoi A, McCrudden KW, Huang J, et al (2003) Human epidermal growth factor receptor signaling contributes to tumor growth via angiogenesis in her2/neu-expressiong experimental Wilms' tumor. J Pediatr Surg 38:1569–1573
20. Amant F, Vloeberghs V, Woestenborghs H, et al (2004) ERBB-2 gene overexpression and amplification in uterine sarcomas. Gynecol Oncol 95:583–587
21. Sawada M, Tsuda H, Kimura M, et al (2003) Different expression patterns of KIT, EGFR, and HER-2 (c-erbB-2) oncoproteins between epithelial and mesenchymal components in uterine carcinosarcoma. Cancer Sci 94:986–991
22. Saffari B, Jones LA, el-Naggar A, et al (1995) Amplification and overexpression of HER-2/neu (c-erbB2) in endometrial cancers: correlation with overall survival. Cancer Res 55:693–5698
23. Sato O, Wada T, Kawai A, et al (2005) Expression of epidermal growth factor receptor, ERBB2 and KIT in adult soft tissue sarcomas: a clinicapathologic study of 281 cases. Cancer 103:1881–1890
24. Sonia L, Ezzat S, Zheng L, et al (1998) Cytoplasmic staining of erbB-2 not mRNA levels correlates with differentiation in human thyroid neoplasia. Clinical Endocrinol 49:629–637
25. Akslen LA, Varhaug JE (1995) Oncoproteins and tumor progression in papillary thyroid. Cancer 76:1643–1654
26. Nuciforo PG, Pellegrini C, Fasani R, et al (2003) Molecular and immunohistochemical analysis of HER2/neu oncogen. Hum Pathol 34:639–645
27. Akiyama T, Sudo C, Ogawara H, et al (1986) The product of the human c-erbB-2 gene: a 185-kilodalton glycoprotein with tyrosine kinase activity. Science 232:1644–1646
28. Fukushige S, Matsubara K, Yoshida M, et al (1986) Localization of a novel v-erbB-related gene, c-erbB-2, on human chromosome 17 and its amplification in a gastric cancer cell line. Mol Cell Biol 6:955–958
29. Matth L, Bianchi F, Prato ID, et al (2001) Renal cell cultures for the study of growth factor interactions underlying kidney organogenesis. In Vitro Cell Dev Biol Anim 37:251–258
30. Bernardini N, Bianchi F, Lupetti M (1996) Immunohistochemical localization of the epidermal growth factor, transforming growth factor-α and their receptor in human mesonephros and metanephros. Dev Dyn 206:31–238
31. Taub M, Wang Y, Szczesny TM (1990) Epidermal growth factor or transforming growth factor α is required for kidney tubulogenesis in matrigel cultures in serum-free medium. Proc Natl Acad Sci USA 87:4002–4006
32. Rivera MN, Haber DA (2005) Wilms' tumour: connecting tumorigenesis and organ development in the kidney. Nat Rev Cancer 5:699–712
33. Schmidt D, Beckwith JB (1995) Histopathology of childhood renal tumors. Hematol Oncol Clin North Am 9:1179–1200

Oncogene (2006) 25, 917–928

www.nature.com/onc

ORIGINAL ARTICLE

Hypoxia selects for high-metastatic Lewis lung carcinoma cells overexpressing Mcl-1 and exhibiting reduced apoptotic potential in solid tumors

N Koshikawa[1,2], C Maejima[1], K Miyazaki[3], A Nakagawara[3] and K Takenaga[1]

[1]Division of Chemotherapy, Chiba Cancer Center Research Institute, Chuoh-ku, Chiba, Japan; [2]Division of Pathology, Chiba Cancer Center Research Institute, Chuoh-ku, Chiba, Japan and [3]Division of Biochemistry, Chiba Cancer Center Research Institute, Chuoh-ku, Chiba, Japan

Low oxygen tension (hypoxia) is a common feature of solid tumors and stimulates the expressions of a variety of genes including those related to angiogenesis, apoptosis and endoplasmic reticulum (ER) stress response. Here we show a close correlation between metastatic potential and the resistance to hypoxia- and ER stress-induced apoptosis among the cell lines with differing metastatic potential derived from Lewis lung carcinoma. An apoptosis-specific expression profiling and immunoblot analyses revealed that the expression of antiapoptotic Mcl-1 increased as the resistance to apoptosis increased. Downregulation of the Mcl-1 expression in the high-metastatic cells by Mcl-1 small interfering RNA increased the sensitivity to hypoxia-induced apoptosis and decreased the metastatic ability. The hypoxia-induced apoptosis was not associated with p53 accumulation, although at present it is not possible to conclude that apoptosis-induced apoptosis is p53-independent. There was no correlation between the expression levels of ER stress-response proteins GADD153, GRP78 and ORP150 and the resistance to hypoxia or ER stresses. *In vitro*, small numbers of the high-metastatic cells overtook the low-metastatic cells after exposure to several rounds of hypoxia and reoxygenation. In solid tumors initially established from equal mixtures, the proportion of the high-metastatic cells to low-metastatic cells was significantly higher in hypoxic areas. Moreover, the high-metastatic cells were overtaking the low-metastatic cells in some of the tumors. Thus, tumor hypoxia and ER stress may provide a physiological selective pressure for the expansion of the high-metastatic cells overexpressing Mcl-1 and exhibiting reduced apoptotic potential in solid tumors.
Oncogene (2006) **25**, 917–928. doi:10.1038/sj.onc.1209128; published online 10 October 2005

Keywords: hypoxia; ER stress; apoptosis; Mcl-1; metastasis

Correspondence: Dr K Takenaga, Division of Chemotherapy, Chiba Cancer Center Research Institute, 666-2 Nitona, Chuoh-ku, Chiba 260-8717, Japan.
E-mail: keizo@chiba-cc.jp
Received 6 January 2005; revised 22 August 2005; accepted 22 August 2005; published online 10 October 2005

Introduction

Response to low oxygen tension (hypoxia) is a fundamental biological phenomenon and therefore hypoxia gives rise to a variety of physiological responses at cellular, local and systemic levels. The cells placed under hypoxic conditions activate many genes including those related to cell survival, glycolysis, angiogenesis, erythrocyte production and iron metabolism to adapt the environment (Semenza, 2000, 2002; Harris, 2002). The oxygen sensing mechanisms have been intensively studied and found to involve hypoxia-inducible factors (HIFs) as key regulatory transcription factors that are composed of HIF-α subunit and HIF-β/aryl hydrocarbon receptor nuclear translocator subunit (Semenza, 2000, 2002; Harris, 2002). HIF binds to the hypoxia-responsive element of hypoxia-responsive genes such as vascular endothelial growth factor (VEGF) and proapoptotic Bnip3, a member of the Bcl-2 family (Semenza, 2000, 2002; Harris, 2002).

Most solid tumors harbor areas of hypoxia, both acute and chronic, due to aberrant vasculature formation and high interstitial pressure (Chaplin and Hill, 1995; Brown and Giaccia, 1998). Although most of the tumor cells die in chronic hypoxia, some of them actually can survive for more than several days in a quiescent or the so-called dormant state (Durand and Sham, 1998) and restart to divide once closed vessels reopen or new vasculatures reach the hypoxic areas. It has been shown that hypoxia induces genetic instability, DNA over-replication and gene amplification in a variety of cultured cells (Rice *et al.*, 1986; Russo *et al.*, 1995; Coquelle *et al.*, 1998). A short-term hypoxia followed by reoxygenation transiently enhances invasive and metastatic potential of some tumor cells (Young and Hill, 1990; Graham *et al.*, 1999; Cairns *et al.*, 2001). Tumor hypoxia selects $p53^{-/-}$ transformed cells and thereby expands cells with diminished apoptotic potential *in vitro* (Graeber *et al.*, 1996). These mechanisms all together are likely to influence the malignant progression of tumor cells (Hill, 1990; Russo *et al.*, 1995; Graeber *et al.*, 1996; Coquelle *et al.*, 1998; Dachs and Chaplin, 1998). Besides, since hypoxic tumor cells cease to divide, they are resistant to conventional radiotherapy and chemotherapy (Rice *et al.*, 1986; Young and Hill, 1990; Teicher, 1994).

Physiological endoplasmic reticulum (ER) stress such as glucose starvation is also present in solid tumors. Hypoxia has been shown to upregulate ER stress-response genes including growth arrest/DNA damage-inducible protein 153 (GADD153/CHOP), which is a proapoptotic transcription factor (Friedman, 1996) and ER chaperones such as glucose-regulated protein (GRP)78/BIP (Munro and Pelham, 1986) and oxygen-regulated protein (ORP)150, which are antiapoptotic proteins (Kuwabara *et al.*, 1996). Upregulation of these ER stress proteins is HIF-independent.

There is accumulating evidence that developing resistance to common apoptotic stimuli is one of the factors that confer high metastatic capability to tumor cells (Glinsky and Glinsky, 1996; McConkey *et al.*, 1996; Bufalo *et al.*, 1997; Glinsky, 1997; Inbal *et al.*, 1997; Shtivelman, 1997; Takaoka *et al.*, 1997; Fernandez *et al.*, 2000; Lowe and Lin, 2000; Wong *et al.*, 2001). The apoptosis-resistant phenotype may be advantageous for tumor cells to survive in the metastatic process. We reported that the high-metastatic clone (A11 cells) established from Lewis lung carcinoma is more resistant to apoptosis induced by serum starvation, hypoxia and glucose deprivation than the low-metastatic clone (P29 cells) (Takasu *et al.*, 1999). However, it remained to be examined whether there is a correlation between metastatic ability and resistance to apoptosis induced by various stresses among various clones with differing metastatic potential. In addition, molecular mechanisms of the apoptosis resistance of the high-metastatic cells remained obscure. We addressed here these points and, furthermore, if hypoxia could act as a physiological selective pressure in solid tumors for the expansion of high-metastatic tumor cells that possess diminished apoptotic potential. The results showed that the high-metastatic Lewis lung carcinoma cell lines are more resistant to hypoxia- and ER stress-induced apoptosis than the low-metastatic cell lines, that the high-metastatic cells overexpress antiapoptotic Mcl-1, and that hypoxia selects for the high-metastatic cells in solid tumors.

Results

Correlation between metastatic potential and resistance to hypoxia- and ER stress-induced apoptosis in the low- and high-metastatic cell lines

To investigate the correlation between susceptibility to hypoxia-induced cell death and metastatic potential, we exposed the five cell lines with differing metastatic potential derived from a mouse Lewis lung carcinoma (metastatic capability; P29 = P34 < C2 < D6 < A11) to hypoxia (~0.1% O_2), corresponding to oxygen concentrations commonly found in solid tumors. Cell death was monitored after culturing the cell lines for 72 h under hypoxia. The results showed that only less than 8% of P29 and P34 cells were viable while about 20% of C2 cells and over 45% of D6 and A11 cells remained viable (Figure 1a). Thus, we observed a tendency where the resistance to hypoxia-induced cell death is correlated with the metastatic ability. The time course showed that hypoxia induced cell death more rapidly in P29 cells than in A11 cells (Figure 1b). Clonogenic assays in which the cells were exposed to hypoxia for 3 or 4 days and then reoxygenated to form colonies also demonstrated that A11 cells survived longer than P29 cells under hypoxic conditions (Figure 1c). The cells positive for annexin V and TUNEL staining increased in hypoxic P29 cells (Figure 1d). An increase in the number of cells exhibiting chromatin condensation and fragmentation as assessed by DAPI staining was also observed in hypoxic P29 cells (0.1 and 26.1% for normoxic and hypoxic P29 cells, respectively) (Figure 1d). In addition, flow cytometric analysis revealed an increase in the percentage of sub-G1 population in these cells (0.7 and 20.6% for normoxic and hypoxic cells, respectively) (Figure 1e). Thus, these data indicate that hypoxic P29 cells were dying through apoptosis. We confirmed that hypoxic A11 cells died of apoptosis based on the same criteria.

To test whether the high-metastatic cell lines are also resistant to ER stresses compared with the low-metastatic cell lines, we treated P29, P34, D6 and A11 cells with chemical ER stress inducers for 2 days and examined their viability. As shown in Figure 2, compared to P29 and P34 cells, D6 and A11 cells were much more resistant to apoptosis induced by tunicamycin (5 μg/ml), brefeldin A (5 μg/ml), thapsigargin (250 nM) and A23187 (1 μM).

Mcl-1 is overexpressed in the high-metastatic cell lines

To find out the genes responsible for the susceptibility to hypoxia-induced apoptosis, we compared the expression profile of apoptosis-related genes among normoxic and hypoxic P29 and A11 cells using a cDNA expression microarray cumulated apoptosis-related genes. The data showed that A11 cells expressed antiapoptotic *Mcl-1* gene at higher levels than P29 cells (not shown). Immunoblot analysis confirmed a higher expression of Mcl-1 in A11 cells than in P29 cells under both normoxic and hypoxic conditions (Figure 3A). We detected two close bands (40 and 37 kDa) on the blots. Since the expressions of the bands were decreased by treatment with Mcl-1 siRNA (see below), the 37 kDa band may be a degradation product of Mcl-1 or, though less likely, a splicing variant of *Mcl-1* gene. It is of note that the cell lines expressed Mcl-1 (40 kDa) at the levels according to the resistance to hypoxia- and other stress-induced apoptosis (Figure 3A and B). Consistent with the recent report that hypoxia enhances Mcl-1 expression in hepatoma HepG2 cells through HIF-1 (Piret *et al.*, 2005), the amount of Mcl-1 was increased by hypoxia in C2, D6 and A11 cells (Figure 3B). Immunohistochemistry for Mcl-1 on the sections prepared from paraffin-embedded P29 and A11 tumors showed a higher expression of Mcl-1 in A11 cells than in P29 cells, indicating that Mcl-1 overexpression is persistent even *in vivo* (Figure 3C).

The expression profiling also showed that hypoxia induced proapoptotic *Bnip3* gene expression in both P29

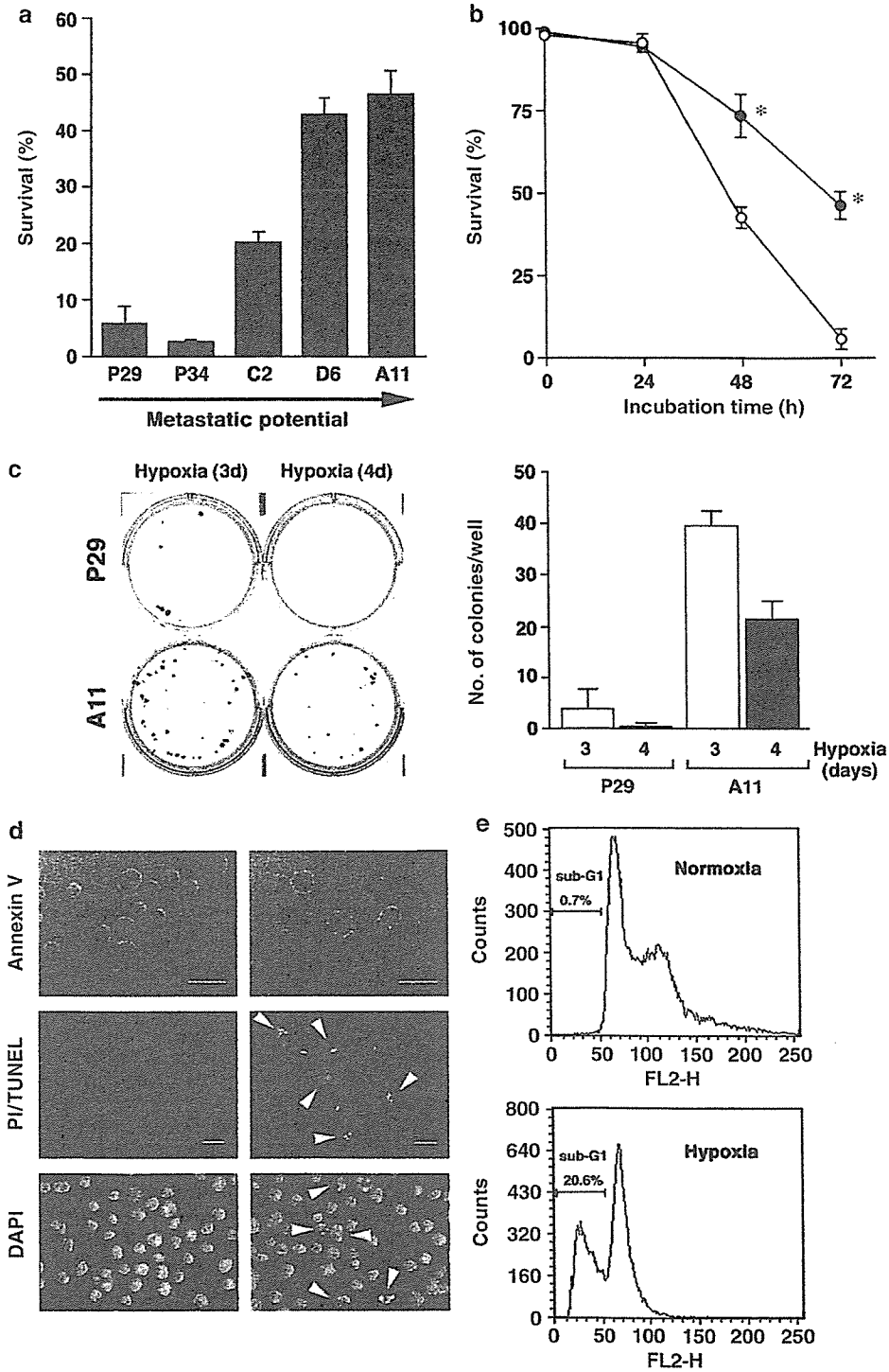

Figure 1 Sensitivity to hypoxia-induced apoptosis of the Lewis lung carcinoma cell lines. (**a**) Hypoxia-induced cell death of the cell lines with differing metastatic potential. The cell lines were exposed to hypoxia for 72 h. Percentage of living cells was determined on the basis of trypan blue exclusion. Bars; s.d. of triplicate determinations. (**b**) Time course of cell death induced by hypoxia. P29 (○) and A11 cells (●) were exposed to hypoxia for the indicated time period. Percentage of living cells was determined on the basis of trypan blue exclusion Bars; s.d. of triplicate determinations. *Significant at $P<0.002$. (**c**) Clonogenic assay of cell survival. P29 and A11 cells (100 cells/well) were cultured under hypoxic conditions for 3 or 4 days followed by culturing under normoxic conditions. Colonies were stained with crystal violet (left panel) and then counted (right panel). Bars; s.d. of triplicate determinations. (**d**) Annexin V, TUNEL and DAPI stainings of normoxic (left panels) and hypoxic P29 cells (right panels). P29 cells were cultured under hypoxic conditions for 18, 27 or 28 h, and then stained for annexin V-EGFP, TUNEL (green) and PI (red), or DAPI, respectively. Arrowheads show apoptotic cells. (**e**) Flow cytometric analysis of DNA fragmentation. P29 cells cultured under hypoxic conditions for 27 h were subjected to FACscan analysis. The percentage of sub-G1 fraction is also shown.

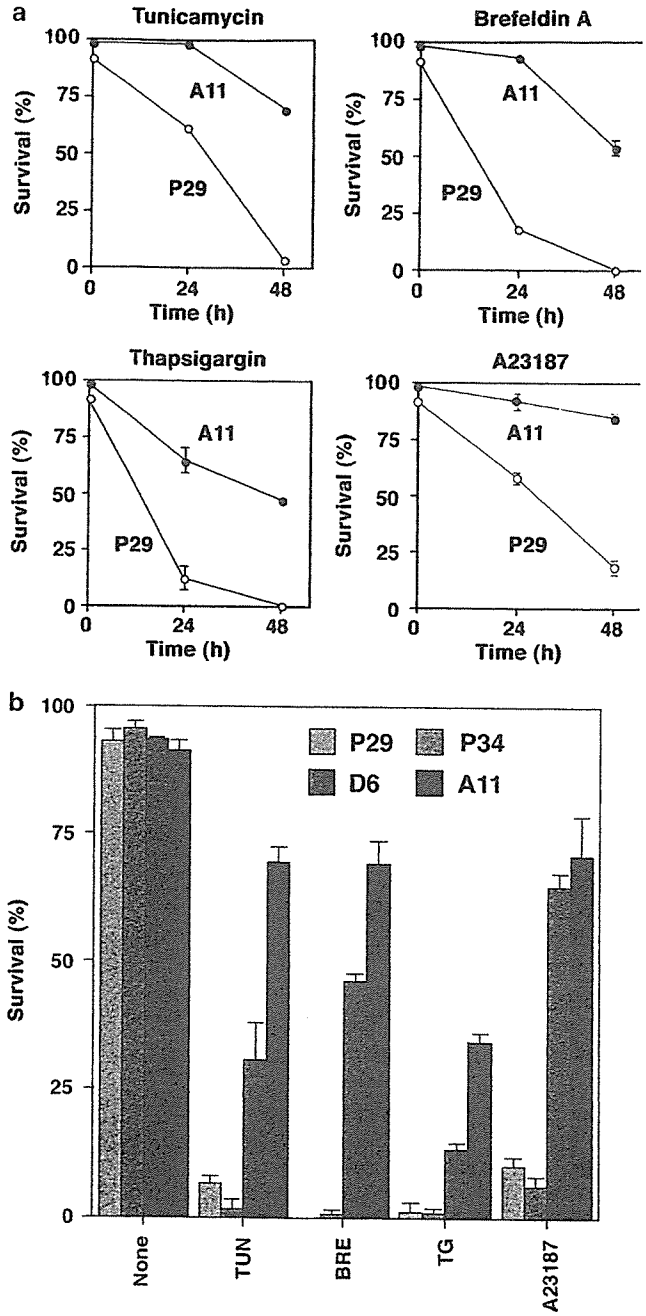

Figure 2 Sensitivity to ER stress-induced apoptosis of the Lewis lung carcinoma cell lines. (**a**) Time course of cell death of P29 (○) and A11 cells (●) exposed to ER stress-inducing agents. The cells were exposed to tunicamycin (5 μg/ml), brefeldin A (5 μg/ml), thaspigargin (250 nM), A23187 (1 μM)). (**b**) Sensitivity of the cell lines with differing metastatic potential to ER stress-inducing agents. P29, P34, D6 and A11 cells were exposed to tunicamycin (5 μg/ml), brefeldin A (5 μg/ml), thaspigargin (250 nM), A23187 (1 μM)) for 2 days. Percentage of living cells was determined on the basis of trypan blue exclusion. Bars; s.d. of triplicate determinations.

and A11 cells (data not shown). Actually, *Bnip3* mRNA expression was induced in all of the cell lines, but the expression level was not correlated with the susceptibility to hypoxia- and other stress-induced apoptosis (Figure 3D).

To investigate whether the hypoxia-induced apoptosis is associated with p53 accumulation, we examined the expression of p53 in hypoxia- and doxorubicin-treated P29, P34, D6 and A11 cells. Immunoblot analysis revealed that hypoxia reduced p53 expression (Figure 3E) and failed to induce endogenous downstream p53 effector proteins, Bax and $p21^{WAF1/CIP1}$, in these cell lines (not shown). By contrast, doxorubicin caused the accumulation of p53 (Figure 3E).

We next compared the expression levels of ER stress-response proteins, GADD153, GRP78 and ORP150, which are known to be induced by hypoxia, between P29 and A11 cells. As shown in Figure 3F and G, the expressions of these proteins were induced by tunicamycin and hypoxia, but there was no difference between 29 and A11 cells.

Effects of Mcl-1 siRNA on hypoxia-induced apoptosis and metastatic potential

To examine if the expression of Mcl-1 is responsible for the resistance to hypoxia-induced apoptosis, we transfected A11 cells with either Mcl-1 siRNA or control siRNA. As shown in Figure 4a and b, the expression of Mcl-1 was suppressed by Mcl-1 siRNA, but not by control siRNA. We then cultured these cells under hypoxic conditions for 60 h and monitored cell death. The results showed that Mcl-1 siRNA-treated A11 cells were more sensitive to hypoxia-induced apoptosis than mock and control siRNA-treated cells in both normal growth medium and serum-starved medium (Figure 4c). Importantly, Mcl-1 siRNA-treated A11 cells were less metastatic than control siRNA-treated cells, as assessed by lung weight and the number of metastatic nodules in the lung (Figure 4d). Thus, it appeared that Mcl-1 is at least in part involved in resistance to hypoxia-induced apoptosis and metastatic potential of A11 cells.

Apoptosis of the low- and high-metastatic cells in hypoxic areas of solid tumors

To examine whether the difference in the susceptibility to hypoxia-induced apoptosis can also be observed *in vivo*, we injected EF5, a nitroimidazole compound, into mice bearing subcutaneous P29 or A11 tumors of nearly equal size for detecting hypoxic areas and stained cryosections of the tumors first with TUNEL assay using fluorescein-labeled nucleotides, and then with Cy3-labeled antibodies against EF5-cellular macromolecule adducts (Figure 5a). EF5 binding occurs under low-oxygen conditions and only in viable cells (Lord *et al.*, 1993). The number of TUNEL-positive cells per 100 μm^2 in EF5-positive (hypoxic) and -negative (normoxic) areas was counted (Figure 5b). We omitted necrotic areas from the investigation. The results showed that the number of apoptotic cells in hypoxic areas of P29 tumors was fourfold larger than that in hypoxic areas of A11 tumors. In normoxic areas, the number of apoptotic cells was small but statistically larger in P29 tumors than in A11 tumors.

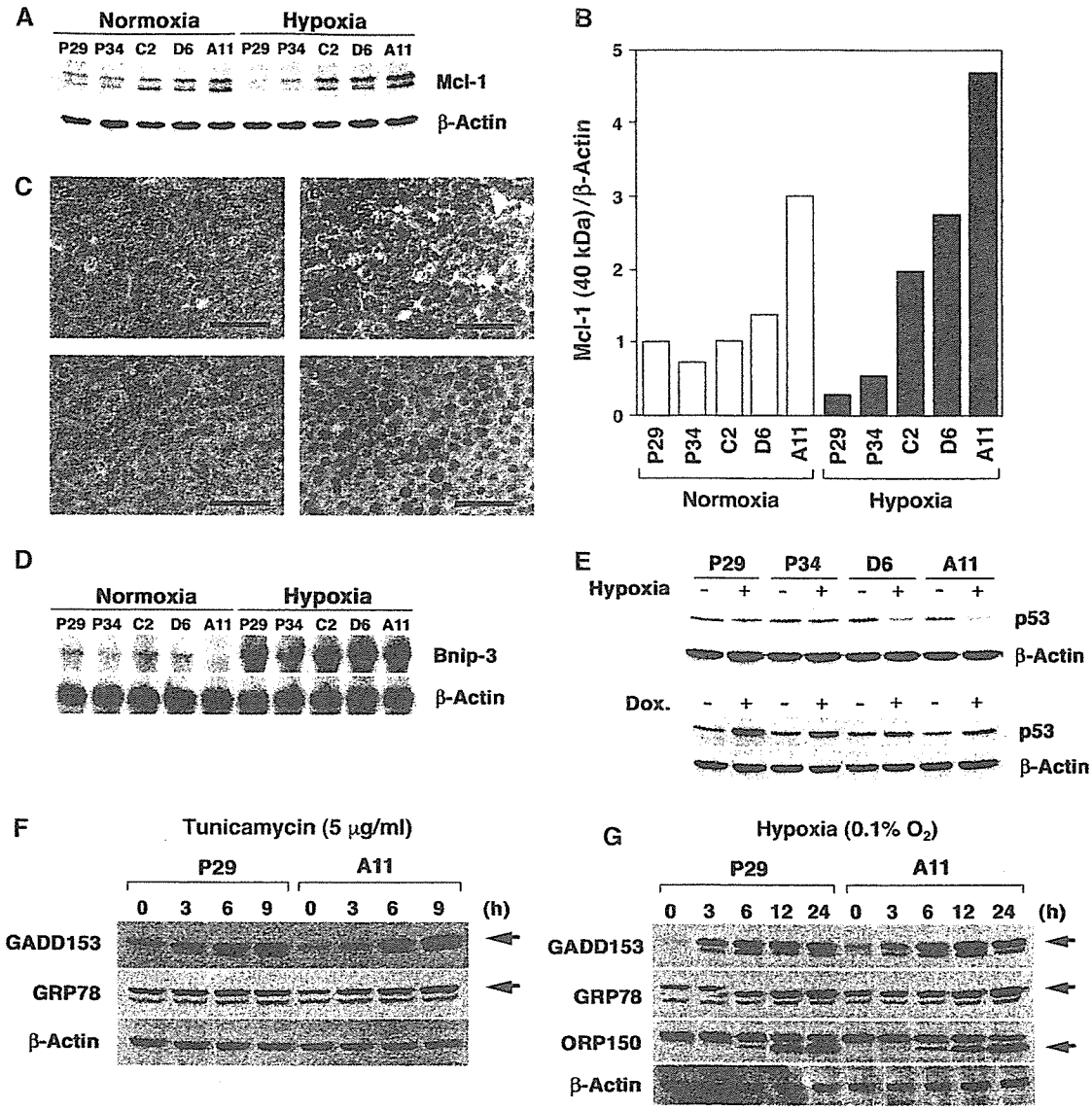

Figure 3 Expressions of apoptosis-related genes in Lewis lung carcinoma cell lines. (**A**) Western blot analysis of the effect of hypoxia on Mcl-1 expression. The cells exposed to hypoxia (~0.1% O_2) for 8 h were subjected to immunoblot analysis for Mcl-1 expression. β-actin served as loading controls. (**B**) Relative values for signal intensity of Mcl-1 (40 kDa) after normalization to the level of β-actin. Scanning densitometry of the gel was performed and the normalized values were represented by the white (under normoxia) and black (under hypoxia) bars. All values are shown as a percentage of the value for normoxic P29 cells. The results are representative of two separate experiments in which similar results were obtained. (**C**) Immunohistochemical analysis of Mcl-1 expression in P29 and A11 tumors. Sections from P29 tumors (a and c) and A11 tumors (b and d) were immunostained with anti-Mcl-1 antibody (a and b) and control IgG (c and d). Bars; 50 μm. (**D**) Effects of hypoxia on *Bnip3* mRNA expression. The cells exposed to hypoxia (0.1% O_2) for 8 h were subjected to Northern analysis for Bnip3 mRNA expression. β-Actin mRNA served as loading controls. (**E**) Western blot analysis of the effects of hypoxia and doxorubicin on the accumulation of p53 protein. The cells exposed to hypoxia (0.1% O_2) for 24 h or 5 μg/ml doxorubicin (Dox) for 20 h were subjected to immunoblot analysis for p53 expression. β-Actin served as loading controls. (**F**) Western blot analysis of the effects of tunicamycin on the expressions of GADD153 and GRP78. P29 and A11 cells were exposed to 5 μg/ml tunicamycin for the indicated periods of time. βActin served as loading controls. (**G**) Western blot analysis of the effects of hypoxia on the expressions of GADD153, GRP78 and ORP150. P29 and A11 cells were exposed to hypoxia (0.1% O_2) for the indicated periods of time. β-actin served as loading controls.

Survival advantage of the high-metastatic cells under hypoxic conditions

The above results prompted us to examine whether A11 cells have a survival advantage over P29 cells under hypoxic conditions. To this end, we established genetically labeled P29 ($P29^{EGFP}$ cells) and A11 cells ($A11^{IRES\text{-}EGFP}$ cells) after selecting P29 and A11 cells stably transfected with pEGFP-N1 and pIRES2-EGFP, respectively (Figure 6a), and characterized their properties. $P29^{EGFP}$ cells grew faster than $A11^{IRES\text{-}EGFP}$ cells *in vivo*, and at 17 days after tumor cell inoculation $P29^{EGFP}$ tumors were twice larger than $A11^{IRES\text{-}EGFP}$ tumors (Figure 6b). $P29^{EGFP}$ tumors contained large necrotic regions. $P29^{EGFP}$ and $A11^{IRES\text{-}EGFP}$ cells were low- and

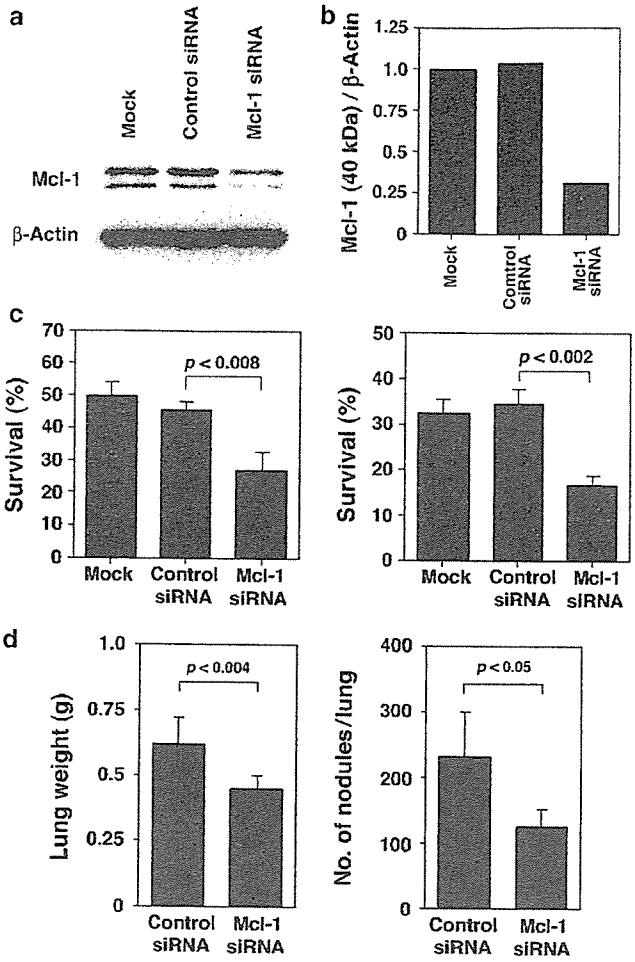

Figure 4 Effects of Mcl-1 siRNA on hypoxia-induced apoptosis and metastatic potential of A11 cells. (**a**) Expression of Mcl-1 in A11 cells treated with Mcl-1 siRNA. A11 cells pretreated with Lipofectamine 2000 alone (mock), 25 nM control siRNA or 25 nM Mcl-1 siRNA for 2 days were subjected to immunoblot analysis for Mcl-1 expression. β-Actin served as loading controls. (**b**) Relative values for signal intensity of Mcl-1 (40 kDa) after normalization to the level of β-actin. Scanning densitometry of the gel was performed and the relative values were represented. All values are shown as a percentage of the value for mock-transfected A11 cells. The results are representative of three separate experiments in which similar results were obtained. (**c**) Sensitivity of Mcl-1 siRNA-treated A11 cells to hypoxia-induced apoptosis. A11 cells pretreated with Lipofectamine 2000 alone (mock), 25 nM control siRNA or 25 nM Mcl-1 siRNA for 2 days were cultured under hypoxic conditions (~0.1% O_2) for 60 h in normal growth medium (left panel) or serum-starved (1% serum) medium (right panel). Cell death was examined by trypan blue staining. Bars; s.d. of triplicate determinations. (**d**) Metastatic potential of Mcl-1 siRNA-treated A11 cells. A11 cells pretreated with 25 nM control siRNA or 25 nM Mcl-1 siRNA for 2 days were injected intravenously into C57BL/6 mice (6 mice/group). At 17 days after the injection, the weight of the lungs (left panel) and the number of metastatic nodules (right panel) were measured. Bars; s.d.

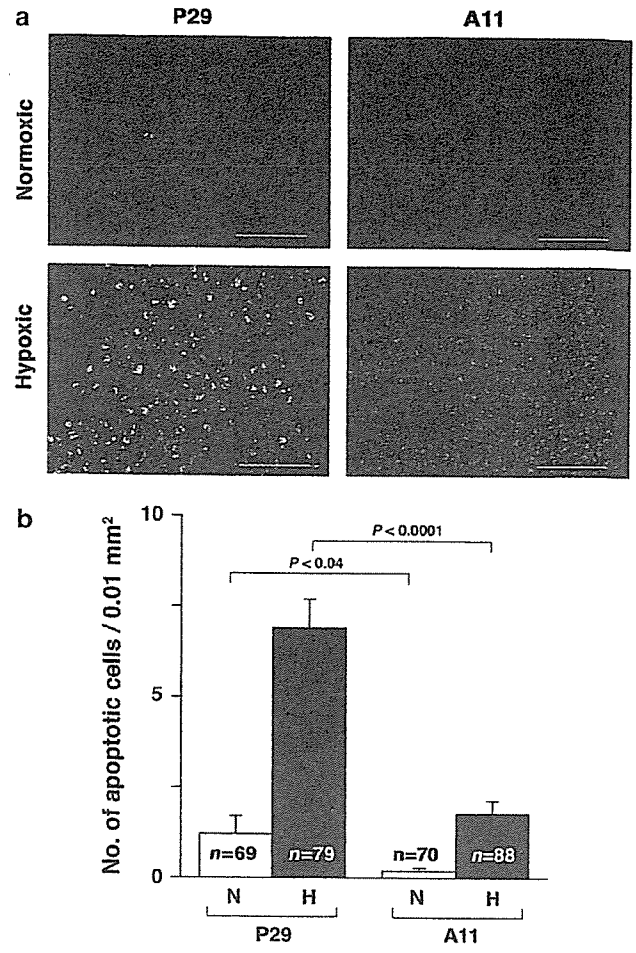

Figure 5 Apoptosis of P29 and A11 cells in tumor hypoxic areas. (**a**) TUNEL staining (green) and EF5 staining (red) of frozen sections of subcutaneous tumors established from P29 and A11 cells. (**b**) Frequency of apoptotic (TUNEL-positive) cells in normoxic (N) and hypoxic (H) areas. Bars; s.e.m.

high-metastatic, respectively, in both experimental and spontaneous metastasis assays (Figure 6c) and showed a similar apoptosis resistance to their parental cells (Figure 6d).

To obtain a standard curve by which the percentage of $A11^{IRES\text{-}EGFP}$ cells in mixtures of unknown proportions of $P29^{EGFP}$ and $A11^{IRES\text{-}EGFP}$ cells could be calculated, we extracted genomic DNA from mixtures of known proportions of the cells and performed PCR followed by Southern blot with an EGFP probe (Figure 6e). By plotting the relative intensities of the bands corresponding to EGFP and IRES-EGFP against the known proportion of $A11^{IRES\text{-}EGFP}$ cells, a standard curve, although slightly sigmoid, was obtained (Figure 6f). The value at each point did not significantly fluctuate even when we carried out PCR under various conditions (1–100 ng DNA, 20–35 PCR cycles) (not shown).

We then mixed $A11^{IRES\text{-}EGFP}$ and $P29^{EGFP}$ cells at a 1:1, 1:10 or 1:100 ratio and treated them with multiple rounds of hypoxia and reoxygenation (recovery in normoxia). The percentage of $A11^{IRES\text{-}EGFP}$ cells at the time of cell harvesting was determined from the standard curve after quantitation of radioactive intensity of the PCR bands. We found that the percentage of $A11^{IRES\text{-}EGFP}$ cells increased dramatically after several rounds of hypoxia-reoxygenation in every case (Figure 7a and b). The intensity of the band corresponding to EGFP and IRES-EGFP in $P29^{EGFP}$ and $A11^{IRES\text{-}EGFP}$

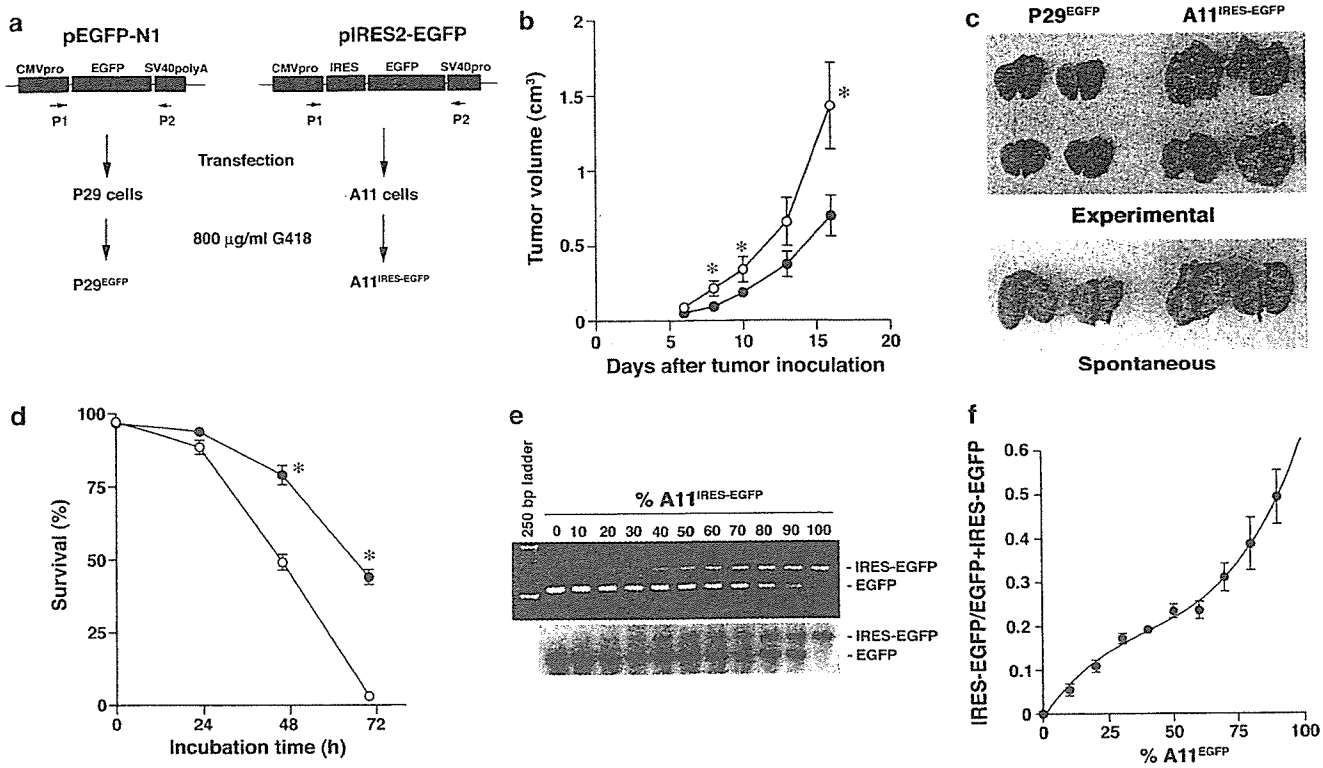

Figure 6 Establishment and properties of P29^{EGFP} and A11$^{IRES\text{-}EGFP}$ cells. (**a**) Schematic drawings of the establishment of P29^{EGFP} and A11$^{IRES\text{-}EGFP}$ cells and the primers, P1 and P2, used for PCR. (**b**) *In vivo* growth of P29^{EGFP} and A11$^{IRES\text{-}EGFP}$ cells. P29^{EGFP} (○) and A11$^{IRES\text{-}EGFP}$ cells (●) (2.5×10^5) were injected subcutaneously into C57BL/6 mice (7 mice/group). Bars; s.e.m. *Significant at $P<0.04$. (**c**) Metastatic potential of P29^{EGFP} and A11$^{IRES\text{-}EGFP}$ cells. For experimental metastasis, the cells (2×10^5 cells/mouse) were injected intravenously, and the lungs were excised 17 days after the injection. For spontaneous metastasis, the cells (2×10^5 cells/mouse) were inoculated subcutaneously, and the lungs were excised 30 days after the inoculation. (**d**) Hypoxia-induced apoptosis of P29^{EGFP} (○) and A11$^{IRES\text{-}EGFP}$ cells (●). Percentage of living cells was determined on the basis of trypan blue exclusion. Bars; s.d. of triplicate determinations. *Significant at $P<0.003$. (**e**) Ethidium bromide staining and Southern blot of PCR fragments amplified using genomic DNA extracted from mixtures of known proportions of P29^{EGFP} and A11$^{IRES\text{-}EGFP}$ cells. (**f**) A standard curve by which the percentage of A11$^{IRES\text{-}EGFP}$ cells in a mixed culture or a tumor could be calculated. The relative intensities of the bands shown in (e) were plotted against the known proportion of A11$^{IRES\text{-}EGFP}$ cells. Bars; s.d. of three independent experiments.

cells, respectively, treated with the same protocol was constant (Figure 7c), indicating that the integrated marker genes was stable.

Survival advantage of the high-metastatic cells in solid tumors

We next examined the proportion of A11$^{IRES\text{-}EGFP}$ cells in normoxic and hypoxic areas of solid tumors established from a 1:1 mixture of P29^{EGFP} and A11$^{IRES\text{-}EGFP}$ cells. Since P29^{EGFP} cells grew faster than A11$^{IRES\text{-}EGFP}$ cells *in vivo* (Figure 6b), the percentage of A11$^{IRES\text{-}EGFP}$ cells in both normoxic and hypoxic areas of the heterogeneous tumors should be lower than 50% if no selection of cells occurs in the tumors. We cut out EF5-negative and -positive areas (approximately total 1 mm^2) from cryosections of the tumors excised at 17 days after tumor inoculation by using laser-assisted microdissection, extracted genomic DNA, and then examined the percentage of A11$^{IRES\text{-}EGFP}$ cells in these areas as described above (Figure 8a and b). The data showed that the proportion of A11$^{IRES\text{-}EGFP}$ cells in normoxic areas decreased from the initial 50% in five out of the seven mixed tumors. However, the proportion was over 70% in #2 and #5 tumors (Figure 8b). Intriguingly, the percentage of A11$^{IRES\text{-}EGFP}$ cells in hypoxic areas was quite high in five out of the seven tumors. Overall, the proportion of A11$^{IRES\text{-}EGFP}$ cells in normoxic and hypoxic areas was 36.4 ± 26.0 and $69.0 \pm 21.0\%$, respectively ($P<0.011$). The intensity of bands corresponding to EGFP and IRES-EGFP of the cells collected from normoxic and hypoxic areas of P29^{EGFP} and A11$^{IRES\text{-}EGFP}$ tumors was constant (Figure 8c), indicating that the integrated marker genes was also stable *in vivo*. Thus, A11$^{IRES\text{-}EGFP}$ cells showed a clear survival advantage over P29^{EGFP} cells in hypoxic areas.

The loss of P29^{EGFP} cells in normoxic areas of some heterogeneous tumors (#2 and #5 tumors) suggests a possibility that a greater portion of P29^{EGFP} cells was lost in the tumors. To test this possibility, we extracted genomic DNA from the whole tumors and examined the proportion of A11$^{IRES\text{-}EGFP}$ cells. The results showed that the proportion was over 90% in #2 tumor, indicating that A11$^{IRES\text{-}EGFP}$ cells nearly overtook P29^{EGFP} cells in this tumor (Figure 8d and e). In #5 tumor, it was below 50%. This and the above results suggest that A11$^{IRES\text{-}EGFP}$

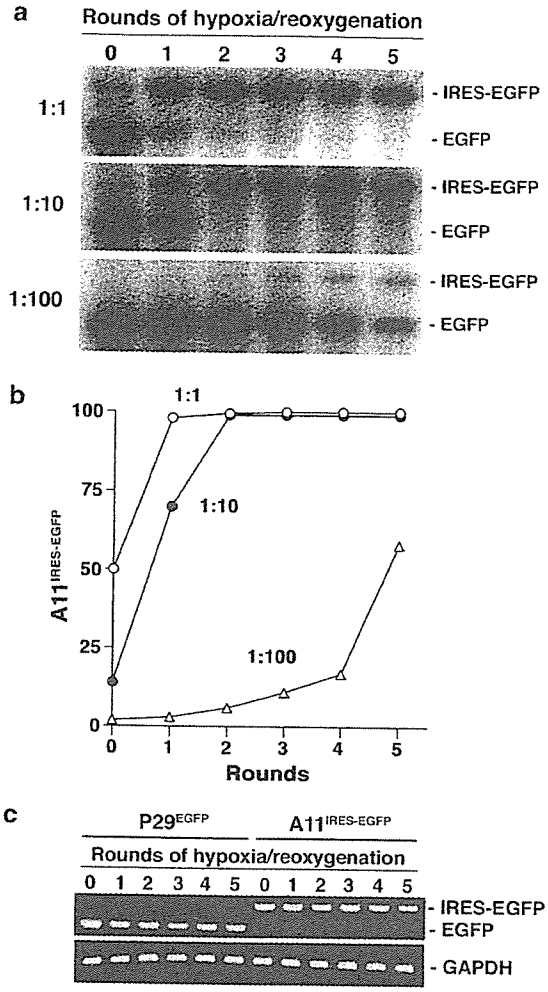

Figure 7 Hypoxia-reoxygenation selects $A11^{IRES\text{-}EGFP}$ cells in a mixed culture. (**a**) Southern blot of PCR fragments amplified using genomic DNA extracted from mixtures of $P29^{EGFP}$ and $A11^{IRES\text{-}EGFP}$ cells. $A11^{IRES\text{-}EGFP}$ were mixed with $P29^{EGFP}$ cells at a 1:1, 1:10 or 1:100 ratio and treated with multiple rounds of hypoxia-reoxygenation. (**b**) Selection of $A11^{IRES\text{-}EGFP}$ cells following hypoxia-reoxygenation treatment. The percentage of $A11^{IRES\text{-}EGFP}$ cells was calculated by the standard curve shown in Figure 6f after measuring the relative intensities of the PCR bands shown in (**a**). The data are representative of two separate experiments in which similar results were obtained. (**c**) Stability of the integrated marker genes in $P29^{EGFP}$ and $A11^{IRES\text{-}EGFP}$ cells. Ethidium bromide staining of the PCR bands is shown.

cells nearly overtook $P29^{EGFP}$ cells only in the local normoxic areas that were dissected by microdissection. The percentage of $A1^{IRES\text{-}EGFP}$ cells was over 50% in #1 and #6 tumors, suggesting that the cells were overtaking $P29^{EGFP}$ cells in these tumors. In other 3 tumors, the percentage was below 50%, indicating that selection of $A11^{IRES\text{-}EGFP}$ cells was occurring in local hypoxic areas of these tumors but was not apparent in whole tumor mass.

Discussion

The data presented here showed a close correlation between metastatic potential and the resistance to hypoxia-induced apoptosis among the cell lines with differing metastatic potential. They also showed that the high-metastatic cells are more resistant to ER stress-induced apoptosis. The hypoxia-induced apoptosis may be p53-independent, because hypoxia neither caused p53 accumulation nor induced the expressions of endogenous downstream p53 effector proteins. An apoptosis-specific expression profiling and immunoblot analyses demonstrated a correlation between the resistance to hypoxia-induced apoptosis and the expression level of Mcl-1. Downregulation of the Mcl-1 expression in A11 cells by Mcl-1 siRNA increased the sensitivity to hypoxia-induced cell death and, importantly, decreased the metastatic ability. Although there are so far few reports directly indicating the involvement of Mcl-1 in metastatic potential of tumor cells, a clinicopathological study suggested Mcl-1 as an indicator of tumor progression and prognosis in patients with gastric carcinoma (Maeta *et al*., 2004). Therefore, Mcl-1 may be one of the factors that confer metastatic potential on at least some tumor cells.

In agreement with the previous reports (Bruick, 2000; Guo *et al*, 2001), hypoxia induced the expression of Bnip3 in all of the cell lines used in this study. Bnip3 is a mitochondrial protein and induces apoptosis independently of Apaf-1, cytochrome *c* release and caspase activation (Vande Velde *et al*., 2000). Bcl-2 and Bcl-X_L bind to Bnip3 and inhibit apoptosis caused by the overexpression of Bnip3 (Ray *et al*., 2000). Therefore, it is possible that Mcl-1 binds to Bnip3 and inhibits Bnip3-induced apoptosis. We preliminarily examined this possibility, and the data showed that Mcl-1 physically interacts with Bnip3 (data not shown).

There was no difference in the inducibility of ER stress- and hypoxia-inducible genes such as GADD153, GRP78 and ORP150 genes between the low- and the high-metastatic cell lines, eliminating the involvement of these genes in the difference of the sensitivity to hypoxia- and ER-stress-induced apoptosis.

The present results clearly demonstrated the survival advantage of A11 cells over P29 cells. In the mixed culture, A11 cells overtook P29 cells during several rounds of hypoxia-reoxygenation. It would be of interest to note that as the rounds of selection proceeded A11 cells progressively became more resistant to apoptosis induced by not only hypoxia but also serum starvation, glucose deprivation and anticancer drugs such as cisplatin and etoposide (not shown). Therefore, it is likely that repeated exposure to hypoxia-reoxygenation results in the selection of not merely A11 cells with original phenotype but of A11 cells with more malignant phenotype, consistent with previous reports (Kim *et al*., 1997; Kinoshita *et al*., 2001).

Coinciding with the *in vitro* experiments, the frequency of apoptosis was greater in the hypoxic areas of A11 tumors than in those of P29 tumors. Intriguingly, it appeared that A11 cells became a majority in the hypoxic areas of many tumor masses established from equal mixtures of P29 and A11 cells. It is of note that although we randomly excised the hypoxic areas the proportion of A11 cells in these areas was over 90% in

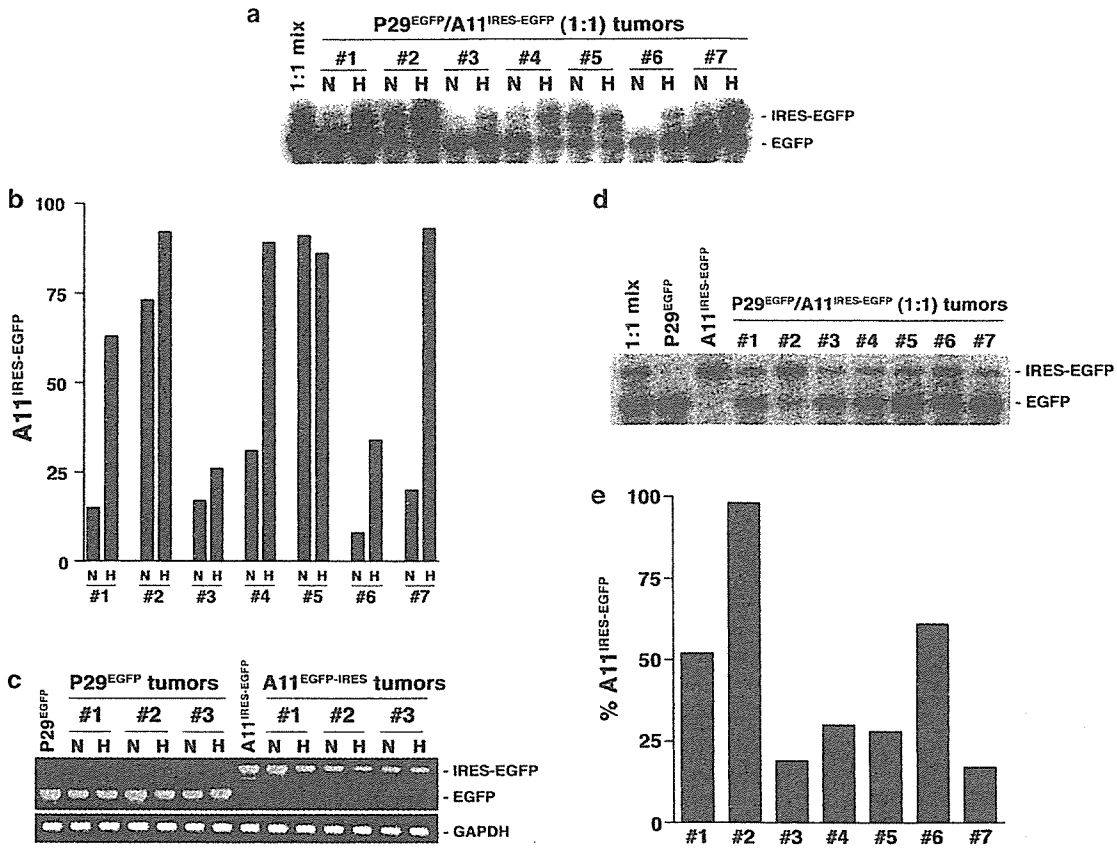

Figure 8 Proportion of $A11^{IRES\text{-}EGFP}$ cells in tumors. (**a**) Southern blot of PCR fragments amplified using genomic DNA extracted from normoxic (N) and hypoxic (H) areas in subcutaneous tumors established from equal mixtures of $P29^{EGFP}$ and $A11^{IRES\text{-}EGFP}$ cells. (**b**) The percentage of $A11^{IRES\text{-}EGFP}$ cells in normoxic (N) and hypoxic (H) areas in subcutaneous tumors. The percentage of $A11^{IRES\text{-}EGFP}$ cells was calculated by the standard curve shown in Figure 5f after measuring the relative intensities of the PCR bands shown in (**a**). (**c**) Stability of the integrated marker genes in normoxic (N) and hypoxic (H) areas of $P29^{EGFP}$ and $A11^{IRES\text{-}EGFP}$ tumors. Ethidium bromide staining of the PCR bands is shown. (**d**) Southern blot of PCR fragments amplified using genomic DNA extracted from subcutaneous tumors established from equal mixtures of $P29^{EGFP}$ and $A11^{IRES\text{-}EGFP}$ cells. (**e**) The percentage of $A11^{IRES\text{-}EGFP}$ cells in subcutaneous tumors. The percentage of $A11^{IRES\text{-}EGFP}$ cells was calculated by the standard curve shown in Figure 6f after measuring the relative intensities of the PCR bands shown in (**d**). Tumor numbers (#) correspond to those in (**a**).

several samples. This was somewhat surprising. We had expected that the proportion would vary widely from one sample to another, because the time of hypoxia influences the degree of apoptosis and EF5-binding does not tell us how long hypoxia had lasted in EF5-positive areas before excision. Nevertheless, a majority of P29 cells was commonly lost in the randomly selected hypoxic areas. One possible explanation for this is that P29 cells die more rapidly in *in vivo* hypoxic areas in which starvation of growth factors and nutrients that could act synergistically with hypoxia to induce apoptosis also occurs. We then exposed P29 and A11 cells to serum starvation (0.5% FBS) and hypoxia (0.1% O_2) simultaneously. The data showed that more than 75% of P29 cells died within 24 h while more than 70% of A11 cells survived. Thus, P29 cells are less tolerant towards severer conditions in *in vivo* hypoxic areas than A11 cells, and this might explain the rapid loss of P29 cells in hypoxic areas. Interestingly, we observed two cases out of the seven tumors in which A11 cells dominated in not only hypoxic areas but also normoxic areas. It is possible that the normoxic areas represent the ones that are reoxygenated after hypoxia. Intriguingly, in one case (#2 tumor), the proportion of A11 cells in the tumor mass was over 90%. This suggests that a majority of P29 cells died of apoptosis induced by severe hypoxia and other microenvironmental factors in the early phase of growth of this tumor, resulting in the selection of A11 cells. The degree of tumor vascularization and angiogenesis may vary from one tumor to another even if they are established from the same tumor cells, and accordingly the extent of hypoxia may differ in individual tumor. This may explain the difference in the proportion of A11 cells in each tumor.

It has been reported that hypoxia induces p53-dependent apoptosis and thus selects $p53^{-/-}$ cells (Graeber *et al*., 1996). Our study showed that hypoxia selects for cells with reduced apoptotic potential and high-metastatic ability. This phenomenon could occur in human tumors such as cervical cancer, head and neck cancer and soft tissue sarcoma in which a correlation between hypoxia and aggressiveness or poor prognosis has been reported (Brizel *et al*., 1996, 1997; Höckel

et al., 1996, 1999). Therefore, the data presented here may have important implications for malignant progression of tumors.

Materials and methods

Cell culture

The cell lines, P29, P34, C2, D6 and A11, established from Lewis lung carcinoma, have been characterized elsewhere (Takasu *et al.*, 1999; Koshikawa *et al.*, 2003). They were grown in Dulbecco's modified Eagle's medium (DMEM) containing 10% fetal bovine serum supplemented with 100 units/ml penicillin and 100 μg/ml streptomycin. Cells were cultured at 37°C in a humidified atmosphere with 5% CO_2 or under hypoxic conditions (ca. 0.1% O_2) generated in BBL GasPak Pouch (Becton Dickinson Microbiology Systems, Cockeysville, MA, USA). In some experiments, they were treated with tunicamycin (Sigma-Aldrich, St Louis, MO, USA), brefeldin A (WAKO Pure Chemical Industries, Ltd., Osaka, Japan), thapsigargin (Sigma-Aldrich), A23187 (Sigma-Aldrich) or vehicle alone.

Assessment of cell viability and apoptosis

Cells were seeded at a concentration of 3×10^5 cells/dish (Falcon 3002), and cell death was induced by culturing them under hypoxic conditions or in the presence of various drugs. For aerobic recovery, the cells were cultured in normoxia until they become subconfluent, thus the recovery time was different for each cell line. Cell viability was assessed by trypan blue dye exclusion. Flow cytometric analysis was performed as described previously (Takasu *et al.*, 1999) to detect cellular DNA fragmentation with a FACScan flow cytometer (Becton Dickinson, Mountain View, CA, USA). Chromatin condensation and fragmentation were visualized by staining the cells with DAPI (10 μg/ml). Annexin V and terminal deoxynucleotidyl transferase-mediated deoxyuridine triphosphate nick-end labeling (TUNEL) stainings were carried out using Annexin V-EGFP Apoptosis Detection Kit (MBL, Nagoya, Japan) and ApopTag Fluorescein *In situ* Apoptosis Detection Kit (Serologicals Corp., Norcross, GA, USA), respectively, according to the manufacturer's instructions. The fluorescence was observed under a Fluoview confocal laser microscope (Olympus, Tokyo, Japan). For clonogenic assay, cells were seeded at a concentration of 100 cells/well of six-well plates (Falcon 3046), incubated for 3 or 4 days under hypoxic (~0.1% O_2) conditions, and then allowed to grow under normoxic conditions for 8–10 days. Colonies were fixed with methanol and stained with 0.05% crystal violet.

Expression profiling of apoptosis-related genes

Expressions of apoptosis-related genes in normoxic and hypoxic P29 and A11 cells were carried out using Mouse Apoptosis GEArray Q™ series containing a panel of 96 key genes involved in apoptosis (SuperArray, Inc., Bethesda, MD, USA). Hybridization of the microarray with a biotin-16-dUTP-labeled cDNA probe and chemiluminescent detection were performed according to the manufacturer's instructions.

Northern blot analysis

Total RNA was electrophoresed on 1% agarose gel containing formaldehyde and transferred to nylon filters. Blots were hybridized with a ^{32}P-labeled mouse *Bnip3* cDNA probe that was prepared by RT–PCR.

Small interfering RNA (siRNA) transfection

Mcl-1 siRNA (Santa Cruz Biotechnologies, Inc., Santa Cruz, CA, USA) or Silencer Negative Control #1 siRNA (Ambion, Inc., Austin, TX, USA) was transfected into A11 cells with Lipofectamine 2000 (Invitrogen, Carlsbad, CA, USA) according to the manufacturer's protocol. At 3 days after transfection, the cells were subjected to immunoblot analysis for Mcl-1 expression, apoptosis assay and metastasis assay.

Immunoblot analysis

Cells were lysed in 1% Triton X-100, 1% sodium deoxycholate, 0.1% SDS, 50 mM Tris-HCl, pH 7.5, 150 mM NaCl, 1 mM PMSF and protease inhibitor cocktail (Sigma-Aldrich) or directly dissolved in SDS sample buffer. After centrifugation at 10 000 *g* for 10 min at 4°C, the supernatant was used for immunoblot analysis. Proteins were separated by SDS–PAGE under reducing conditions and transferred to a nitrocellulose membrane. The membrane was incubated with first antibodies, washed extensively with TBS-T, and then with species-appropriate HRP-conjugated secondary antibodies. The first antibodies used were anti-p53 antibody (Ab-3, Calbiochem-Novabiochem, Germany), anti-Mcl-1 antibody (Santa Cruz Biotechnology, Inc.), anti-GADD153 antibody (Santa Cruz Biotechnology, Inc.), anti-GRP78 antibody (Santa Cruz Biotechnology, Inc.), anti-ORP180 antibody (IBL, Fujioka, Japan) and anti-β-actin antibody (Sigma-Aldrich). Immunodetection was performed using the enhanced chemiluminescence system (ECL; Amersham Biosciences Corp., Piscataway, NJ, USA). The image of the bands was acquired with an imaging densitometer, and the signal intensities were analyzed with an NIH Image 1.63 software on a Machintosh computer. All signals were normalized to β-actin.

Tumor growth and metastasis assays

Cells (2×10^5 cells/mouse) were inoculated into the abdominal flank of age-matched female C57BL/6 mice (Nippon SLC, Hamamatsu, Japan). Subcutaneous tumor growth was monitored by caliper measurement of two diameters at right angles, and the tumor mass was estimated from the equation volume $= 0.5 \times a \times b^2$, where a and b are the larger and smaller diameters, respectively. For spontaneous metastasis assay, the mice were killed 30 days after tumor cell inoculation, and their lungs were removed. For experimental metastasis assay, tumor cells (2×10^5 cells/mouse) were injected intravenously, and the lungs were removed 17 days later. The lungs were fixed in Bouin's solution and the parietal metastatic nodules were counted. All animal experiments were performed in compliance with the institutional guidelines for the care and use of laboratory animals.

Immunohistochemistry

Subcutaneous tumors were excised, fixed in 10% buffered formalin and embedded in paraffin wax. Paraffin sections were cut at 6 μm thickness and mounted on the silane-coated glass slides. After routine dewaxing and rehydrating, the sections were incubated in 1 × ChemMate®Target Retrieval Solution (DakoCytomation, Glostrup, Denmark) at 121°C for 15 min and rinsed with Dulbecco's phosphate-buffered saline (DPBS). For quenching endogenous peroxidase activity, the sections were incubated in 0.3% H_2O_2 in methanol for 30 min. Thereafter, they were incubated with diluted normal goat serum for 20 min at room temperature and then incubated with anti-Mcl-1 antibody or normal rabbit IgG (4 μg/ml) diluted in ChemMate® Antibody Diluent (DaKoCytomation) containing 2% dry milk at 4°C for 16 h. Immunostaining was carried out by using VECTASTAIN® ABC Kit according to the

manufacturer's instructions. The sections were washed with DPBS and finally counterstained with hematoxylin.

Detection and microdissection of hypoxic areas in tumors
In all, 300 μl of EF5 solution (3 mg/ml) was injected intraperitoneally into mice bearing subcutaneous tumors (Inbal *et al.*, 1997). After 1 h, tumors were surgically removed and frozen in OCT compound. Cryostat sections cut at 10 μm were fixed with 4% paraformaldehyde and washed with DPBS. The sections were treated with 5% mouse serum, 20% dry milk and 0.3% Tween 20 in DPBS overnight at 4°C to block nonspecific binding sites. They were rinsed with 0.3% Tween 20 in DPBS and then incubated with Cy3-labeled monoclonal anti-EF5 antibody (ELK3-51) for 4 h at 4°C. After extensive washing with DPBS, tissue samples were observed under a confocal laser microscope or a fluorescence microscope. For detection of apoptotic cells *in vivo*, TUNEL staining was performed followed by EF5 staining. In some experiments, EF5 binding-positive (hypoxic) and adjacent EF5 binding-negative (normoxic) areas in tumor tissues were dissected using a laser-assisted microdissection system (Leica Microsystems, Tokyo, Japan).

Establishment of cells transfected with pEGFP-N1 or pIRES2-EGFP plasmid
P29 and A11 cells were transfected with pEGFP-N1 and pIRES2-EGFP (BD Biosciences Clontech, Tokyo, Japan), respectively, using Lipofectin reagent (Invitrogen, Tokyo, Japan). After selecting the transfected P29 or A11 cells in the presence of 800 μg/ml G418, a clone designated $P29^{EGFP}$ or $A11^{IRES\text{-}EGFP}$, respectively, was established. They were routinely cultured in the presence of 400 μg/ml G418.

DNA isolation, PCR and Southern blotting
Genomic DNA was extracted from $P29^{EGFP}$, $A11^{IRES\text{-}EGFP}$, mixed cells, solid tumors or microdissected sections by conventional method, treated with RNase A (10 μg/ml) and phenol extracted again. PCR was performed using 1–100 ng genomic DNA and *r*Taq DNA polymerase (TOYOBO Biochemicals, Osaka, Japan) on a Perkin Elmer GeneAmp PCR System 9700. The sense primer (P1) was 5′-AAC TCCGCCCCATTGACGC-3′ corresponding to the sequence within the CMV promoter, and the antisense primer (P2) was 5′-ACAAACCACAACTAGAATGCAG-3′ corresponding to the sequence in the SV40polyA signal. These primers were designed to amplify the EGFP sequence in pEGFP-N1 plasmid and the IRES-EGFP sequence in pIRES2-EGFP plasmid, thus yielding 1118 and 1693 bp PCR products, respectively. The PCR conditions were 94°C for 3 min, followed by 20–30 cycles of 94°C for 30 s, 55°C for 30 s and 72°C for 1 min. The resulting PCR products were electrophoresed on 1.2% agarose gels, transferred to nylon membranes and hybridized with a ^{32}P-labeled *EGFP* cDNA. The membranes were washed and radioactive intensity corresponding to the EGFP and IRES-EGFP bands was quantitated using a Fluoro Image Analyzer FLA-5000 (FUJIFILM, Tokyo, Japan). The measured percentage of $A11^{IRES\text{-}EGFP}$ cells was determined by dividing the intensity of the IRES-EGFP band by the total intensity of the EGFP plus IRES-EGFP bands. The actual percentage of $A11^{IRES\text{-}EGFP}$ cells in a mixed culture and in a tumor was determined from a standard curve established from Figure 6f.

Acknowledgements
We thank the National Cancer Institute (CTEP) for providing EF5. This work was supported in part by Grant-in-Aid from the Ministry of Health, Labour, and Welfare for Third Term Comprehensive Control Research for Cancer and from the Ministry of Education, Culture, Sports, Science and Technology.

References

Brizel DM, Scully SP, Harrelson JM, Layfield LJ, Bean JM, Prosnitz LR *et al.* (1996). *Cancer Res* **56**: 941–943.
Brizel DM, Sibley GS, Prosnitz LR, Scher RL, Dewhirst MW. (1997). *Int J Radiat Oncol Biol Phys* **38**: 285–289.
Brown JM, Giaccia AJ. (1998). *Cancer Res* **58**: 1408–1416.
Bruick RK. (2000). *Proc Natl Acad Sci USA* **97**: 9082–9087.
Bufalo DD, Biroccio A, Leonetti C, Zupi G. (1997). *FASEB J* **11**: 947–953.
Cairns RA, Kalliomaki T, Hill RP. (2001). *Cancer Res* **61**: 8903–8908.
Chaplin DJ, Hill SA. (1995). *Br J Cancer* **71**: 1210–1213.
Coquelle A, Toledo F, Stern S, Bieth A, Debatisse M. (1998). *Mol Cell* **2**: 259–265.
Dachs GU, Chaplin DJ. (1998). *Semin Radiat Oncol* **8**: 208–216.
Durand RE, Sham E. (1998). *Int J Radiat Oncol Biol Phys* **42**: 711–715.
Fernandez Y, Espana L, Manas S, Fabra A, Sierra A. (2000). *Cell Death Differ* **7**: 350–359.
Friedman AD. (1996). *Cancer Res* **56**: 3250–3256.
Glinsky GV. (1997). *Crit Rev Oncol Hematol* **25**: 175–186.
Glinsky GV, Glinsky VV. (1996). *Cancer Lett* **101**: 43–51.
Graeber TG, Osmanian C, Jacks T, Housman DE, Koch CJ, Lowe SW *et al.* (1996). *Nature* **379**: 88–91.
Graham CH, Forsdike J, Fitzgerald CJ, Macdonald-Goodfellow S. (1999). *Int J Cancer* **80**: 617–623.
Guo K, Searfoss G, Krolikowski D, Pagnoni M, Franks C, Clark K *et al.* (2001). *Cell Death Differ* **8**: 367–376.
Harris AL. (2002). *Nat Rev* **2**: 38–47.
Hill RP. (1990). *Cancer Metastasis Rev* **9**: 137–147.
Höckel M, Schlenger K, Aral B, Mitze M, Schaffer U, Vaupel P. (1996). *Cancer Res* **56**: 4509–4515.
Höckel M, Schlenger K, Höckel S, Vaupel P. (1999). *Cancer Res* **59**: 4525–4528.
Inbal B, Cohen O, Polak-Charcon S, Kopolovic J, Vadai E, Eisenbach L *et al.* (1997). *Nature* **390**: 180–184.
Kim CY, Tsai MH, Osmanian C, Graeber TG, Lee JE, Giffard RG *et al.* (1997). *Cancer Res* **57**: 4200–4204.
Kinoshita M, Johnson DL, Shatney CH, Lee YL, Mochizuki H. (2001). *Int J Cancer* **91**: 322–326.
Koshikawa N, Iyozumi A, Gassmann M, Takenaga K. (2003). *Oncogene* **22**: 6717–6724.
Kuwabara K, Matsumoto M, Ikeda J, Hori O, Ogawa S, Maeda Y *et al.* (1996). *J Biol Chem* **271**: 5025–5032.
Lord EM, Harwell L, Koch CJ. (1993). *Cancer Res* **53**: 5721–5726.
Lowe SW, Lin AW. (2000). *Carcinogenesis* **21**: 485–495.
Maeta Y, Tsujitani S, Matsumoto S, Yamaguchi K, Tatebe S, Kondo A *et al.* (2004). *Gastric Cancer* **7**: 78–84.
McConkey DJ, Greene G, Pettaway CA. (1996). *Cancer Res* **56**: 5594–5599.
Munro S, Pelham HR. (1986). *Cell* **46**: 291–300.

Piret JP, Minet E, Cosse JP, Ninane N, Debacq C, Raes M *et al.* (2005). *J Biol Chem* **280**: 9336–9344.
Ray R, Chen G, Vande Velde C, Cizeau J, Park JH, Reed JC *et al.* (2000). *J Biol Chem* **275**: 1439–1448.
Rice GC, Hoy C, Schimke RT. (1986). *Proc Natl Acad Sci USA* **83**: 5978–5982.
Russo CA, Weber TK, Volpe CM, Stoler DL, Petrelli NJ, Rodriguez-Bigas M *et al.* (1995). *Cancer Res* **55**: 1122–1128.
Semenza GL. (2000). *Crit Rev Biochem Mol Biol* **35**: 71–103.
Semenza GL. (2002). *Trends Mol Med* **8**: S62–S67.
Shtivelman E. (1997). *Oncogene* **14**: 2167–2173.
Takaoka A, Adachi M, Okuda H, Sato S, Yawata A, Hinoda Y *et al.* (1997). *Oncogene* **14**: 2871–2977.
Takasu M, Tada Y, Wang JO, Tagawa M, Takenaga K. (1999). *Clin Exp Metastasis* **17**: 409–416.
Teicher BA. (1994). *Cancer Metastasis Rev* **13**: 139–168.
Vande Velde C, Cizeau J, Dubik D, Alimonti J, Brown T, Israels S *et al.* (2000). *Mol Cell Biol* **20**: 5454–5468.
Wong CW, Lee A, Shientag L, Yu J, Dong Y, Kao G *et al.* (2001). *Cancer Res* **61**: 333–338.
Young SD, Hill RP. (1990). *J Natl Cancer Inst* **82**: 371–380.

Biology of Neuroblastomas That Were Found by Mass Screening at 6 Months of Age in Japan

Yasuhiko Kaneko, MD,[1]* Hirofumi Kobayashi, MD,[1] Naoki Watanabe, MD,[1] Nobumoto Tomioka, MD,[1,2] and Akira Nakagawara, MD[2]

Background. Mass screening (MS) of neuroblastoma has been carried out by measuring the urinary catecholamine metabolites in infants at the age of 6 months in Japan. We assessed the incidence of neuroblastoma that may be a target for MS by studying tumor biology. ***Procedure.*** FISH on chromosome 1 and MYCN analysis was performed on 453 patients that were classified into three clinical groups (287 infants found by MS, 51 infants <12 months diagnosed clinically, and 115 children ≥12 months diagnosed clinically). The relationship between the biological types of tumors and the clinical outcome was examined. ***Results.*** Type 1 (trisomy 1 and normal MYCN), type 2 (disomy 1/tetrasomy 1 and normal MYCN), and type 3 (disomy 1/tetrasomy 1 and amplified MYCN) tumors were found in 88.2%, 10.5%, and 1.4% of infants found by MS, in 68.0%, 24.0%, and 8.0% of infants diagnosed clinically, and in 23.4%, 42.3%, and 34.2% of children diagnosed clinically ($P < 0.001$). Infants with type 1 tumors found by MS or diagnosed clinically had earlier stages of the disease ($P < 0.0001$ and $P = 0.0005$) and better overall survival ($P < 0.001$ and $P = 0.005$) than children with type 1 tumors diagnosed clinically. Infants with type 2 tumors found by MS, had earlier stages ($P = 0.06$ and $P < 0.0001$) and better overall survival ($P = 0.014$ and $P < 0.001$) than infants or children with type 2 tumors diagnosed clinically. All three clinical groups of patients with type 3 tumors had advanced stages and dismal prognoses. ***Conclusions.*** About 12% of tumors found by MS showed unfavorable biological (types 2 and 3) characteristics. Pediatr Blood Cancer 2006;46:285–291.

Key words: constitution of chromosome 1; mass screening; neuroblastoma; ploidy

INTRODUCTION

Neuroblastoma is one of the most common solid tumors in childhood and is characterized by a broad spectrum of clinical behaviors [1]. Because of the favorable prognosis of neuroblastomas in infants and the difficulty in curing disseminated neuroblastomas in children 12 months or over, a mass screening (MS) program has been carried out for infants in Japan and some other countries by measuring urinary catecholamine metabolites based on the assumption that early detection of the tumor in infants could improve the overall prognosis of patients [2–4].

Epidemiological studies have recently been published from Quebec, Germany, and Japan [3–6]. The methods of detecting urinary catecholamine metabolites, the time of screening, and the study designs were different among the programs. Although an increase in the incidence of neuroblastoma was seen in all the screening programs, no reduction of mortality was seen in the Quebec and German studies, and a modest decrease in mortality was reported in the Japanese studies.

We previously reported that while neuroblastomas found by MS were characterized by early stages of the disease, triploidy, and a low incidence of *MYCN* gene amplification or 1p deletion, those found clinically at 12 months or over were characterized by advanced stages, diploidy or tetraploidy, and a high incidence of *MYCN* gene amplification and 1p deletion [7,8]. These findings may suggest the limited efficacy of the program.

To clarify the biological characteristics of neuroblastomas that were found by MS, we extended the previous study using interphase fluorescent in situ hybridization (FISH) analysis by increasing the number of tumors, by newly including the tumors found clinically before 12 months of age, and by adding flow cytometric analysis. We here report the biological features of the largest number of neuroblastomas that were found by MS, and that about 12% of tumors found by MS showed poor

DOI 10.1002/pbc.20496
Published online 2 August 2005 in Wiley InterScience (www.interscience.wiley.com)

[1]Division of Cancer Diagnosis, Research Institute for Clinical Oncology and Department of Hematology, Saitama Cancer Center, Saitama, Japan

[2]Division of Biochemistry, Chiba Cancer Center Research Institute, Chiba, Japan

Grant sponsor: Grant-in-Aids for Second-Term Comprehensive 10-Year Strategy for Cancer Control and Scientific Research in the Ministry of Health, Labor and Welfare of Japan; Grant number: H16-KODOMO-012.

*Correspondence to: Yasuhiko Kaneko, Division of Cancer Diagnosis, Research Institute for Clinical Oncology, Saitama Cancer Center, 818 Komuro Ina, Saitama, Japan 362-0806.
E-mail: kaneko@cancer-c.pref.saitama.jp

Received 30 December 2004; Accepted 3 May 2005

prognostic factors that characterize the tumors found in older children with unfavorable prognoses [7,8].

PATIENTS AND METHODS

Patients and Specimens

Tumors that were obtained from 453 Japanese infants or children with neuroblastoma who underwent biopsy or surgery between January 1985 and December 1998. The tumors were sent to the Saitama Cancer Center for cytogenetic and FISH analysis. Two hundred and eighty-seven infants were found by MS to have neuroblastoma at 6 months of age, 51 infants less than 12 months of age, and 115 children 12 months or over were diagnosed clinically. During the same period, 1,896 infants were found by MS to have the tumor in Japan [9], and the 287 MS-positive patients constituted 15.1% of these 1,896 patients. Infants found by MS ranged in age from 6 to 18 months with a median age of 7 months; it took at least 1 month from the screening to the diagnosis of neuroblastoma, infants diagnosed clinically from 6 days to 10 months with a median age of 2 months, and children diagnosed clinically from 13 months to 21 years with a median age of 34 months. Most infants diagnosed clinically did not undergo MS, and most children diagnosed clinically underwent MS with a negative result, but the exact numbers of each category of patients could not be determined. Of the 287 infants found by MS, 269 (94%) were examined by the quantitative measurement of VMA/creatinine (Cre) and homovanillic acid (HVA)/Cre by high-performance liquid chromatography (HPLC) that was used after 1988, and 18 by qualitative assessment of urinary vanillylmandelic acid (VMA) used before 1988. Informed consent was obtained from patients and/or their parents, and the study was approved by the ethics committee of the Saitama Cancer Center. All tumors were histologically classified as neuroblastoma or ganglioneuroblastoma. Patients were staged according to the INSS staging system [10]. Patients of any age with stage 1 or 2 disease, and those less than 12 months with stage 3 disease were treated with either surgery or surgery plus chemotherapy consisting of cyclophosphamide and vincristine, and those 12 months or older with stage 3 or 4 disease, and those less than 12 months with stage 4 disease were treated according to the protocol by the Japanese Neuroblastoma Study Group [11].

Interphase FISH and MYCN Copy Number Analyses

Pathologists in each institution verified that each sample contained 50% or more tumor cells. One half of each sample was used for cytogenetic, FISH, and *MYCN* copy number analyses. The results of the cytogenetic analysis were incorporated in the results of the FISH analysis. To detect the copy number of chromosome 1 s and the status of 1p, we used repetitive DNA probes, D1Z1 (pUC1.77) and D1Z2 (p1-79), specific for the pericentromeric region (1q12) and the sub-telomeric region (1p36.33), respectively. Two-color FISH using the two probes was performed as described previously [8]. Disomy 1, trisomy 1, tetrasomy 1, or pentasomy 1 was determined on the basis of the number of the D1Z1 signals, and 1p deletion was defined when the number of the D1Z2 signals was less than the number of the D1Z1 signals. The results of FISH analysis on 170 of the 453 tumors have been reported previously [8].

Tumors were classified into four cytogenetic groups on the basis of the constitution of chromosome 1, i.e., disomy 1 with no deletion of the short arm (Dis1Norm1p group), disomy 1 with the short-arm deletion (Dis1Del1p group), trisomy 1 with no deletion of the short arm (Tris1Norm1p group), and trisomy 1 with the short-arm deletion (Tris1Del1p group). Tris1 tumors included tumors with trisomy 1 and those with a mixed population of cells with trisomy 1 and cells with tetrasomy 1, with or without cells having pentasomy 1 (Fig. 1). Dis1 tumors included tumors with disomy 1 and those with tetrasomy 1. The tumors were assigned to one of the four cytogenetic groups on the basis of the abnormal tumor-cell population dominating in the 100 cells examined (i.e., $\geq$50%). If tumors had a mixed population of cells with trisomy 1 and cells with tetrasomy 1, each group of cells should occupy at least 25% of the 100 cells counted.

DNA preparation, digestion, and Southern blot analysis using the *MYCN* probe were performed as described previously [8]. More than three copies of the *MYCN* gene

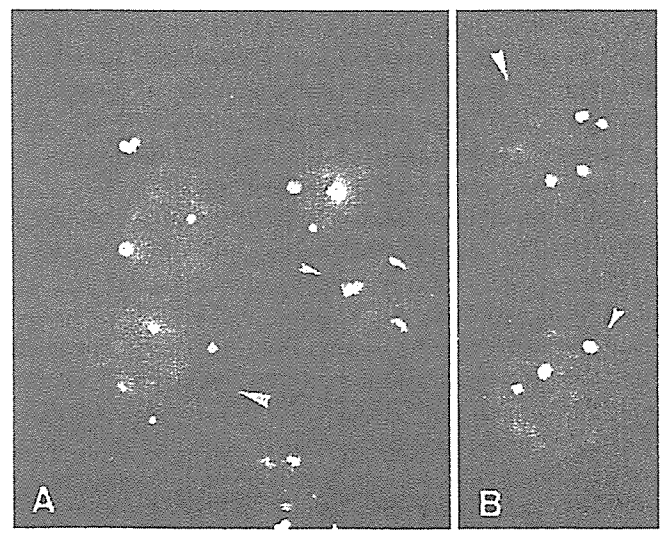

Fig. 1. Interphase FISH analysis using a chromosome 1 probe (D1Z1) on Tris1 tumors with a mixed population of cells with trisomy 1 and tetrasomy 1, with or without pentasomy 1. Cells in A and those in B were derived from 2 different tumors. Large and small arrowheads show cells with tetrasomy 1 and cells with trisomy 1, respectively.

per haploid genome were considered to indicate amplification. Tumors were also classified into three biologic types by the number of chromosome 1 and *MYCN* status; i.e., type 1 (Tris1 and normal *MYCN* copy number), type 2 (Dis1 and normal *MYCN* copy number), and type 3 (Dis1 and amplified *MYCN* copy number) [12,13].

Flow Cytometry

Of 453 neuroblastomas examined by FISH, 134 were also examined by flow cytometry. The DNA index was analyzed on the Becton-Dickinson FACScan flow cytometer by DNA cell-cycle analysis software-version C.

Statistical Analysis

The significance of the differences in various biological and clinical aspects of the disease among the patient groups was examined by the chi-square or Fisher's exact test. The overall survival (OS) for each group of patients was estimated on August 30, 2003 by the Kaplan–Meier method, and compared using log-rank tests. The survival time was defined as the interval between remission induction or surgery and death from any cause.

RESULTS

We examined chromosome 1 by FISH and *MYCN* copy number by Southern blot in all 453 tumors.

Grouping of Neuroblastomas by Constitution of Chromosome 1 and Frequencies of *MYCN* Amplification in Four Cytogenetic Groups

Of the 453 tumors, 56, including 55 with disomy 1 and 1 with tetrasomy 1, were classified as the Dis1 Norm1p tumor, 79, including 58 with disomy 1 and 21 with tetrasomy 1, as the Dis1Del1p tumor, 283, including 192 with trisomy 1 and 91 with a mixed population of the various cells as the Tris1Norm1p tumor, and 35 including 23 with trisomy 1 and 12 with a mixed population of the various cells, as the Tris1Del1p tumor (Table I).

MYCN amplification was found in none of 56 Dis1-Norm1p tumors, 46 of 79 Dis1Del1p tumors, 4 of 283 Tris1Norm1p tumors, and 1 of 35 Tris1Del1p tumors (Table I). Thus, *MYCN* amplification was closely associated with Dis1Del1p tumors. Cytogenetic analysis was successful in two of the five Tris1 tumors with *MYCN* amplification; one showed a modal chromosome number of 62 with three normal chromosome 1 s and the other

TABLE I. Clinical and *MYCN* Features of Four Cytogenetic Groups of Patients Classified by the Constitution of Chromosome 1 in Three Groups of Patients Classified by the Age of Patients and the Method of Tumor Detection

		Stage of disease					*MYCN* amplification		Overall survival at 6 years	
Group of patients	Number of patients	1	2	4S	3	4	+	−	%	Standard error
Infants found by mass-screening										
Dis1Norm1p	18	6	5	4	1	2	0	18	100	
Dis1Del1p	16	5	2	5	0	4	4	12	75.0	10.8
Tris1Norm1p	228	95	62	19	38	14	0	228	99.5	0.4
Tris1Del1p	25	16	4	2	1	2	0	28	100	
Total	287	122	73	30	40	22	4	283	98.2	0.8
Infants diagnosed clinically (<12 months)										
Dis1Norm1p	8	1	1	3	1	2	0	8	87.5	11.7
Dis1Del1p	8	0	1	3	2	2	4	4	37.5	17.1
Tris1Norm1p	34	14	6	7	6	1	1	33	97.1	2.9
Tris1Del1p	1	1	0	0	0	0	0	1	Alive	
Total	51	16	8	13	9	5	5	46	88.0	4.9
Children diagnosed clinically (≥12 months)										
Dis1Norm1p	30	2	3	0	4	21	0	30	58.7	9.1
Dis1Del1p	55	1	3	0	9	42	38	17	38.1	6.8
Tris1Norm1p	21	5	6	0	2	8	3	18	71.4	9.8
Tris1Del1p	9	0	0	0	2	7	1	8	33.3	15.7
Total	115	8	12	0	17	78	42	73	49.0	4.8

Dis1Norm1p, disomy 1/tetrasomy 1 with no 1p deletion; Dis1Del1p, disomy 1/tetrasomy 1 with 1p deletion; Tris1Norm1p, trisomy 1 with no 1p deletion; Tris1Del1p, trisomy 1 with 1p deletion. See the text for more detailed definition. Infants found by MS: Dis1Norm1p, Tris1Norm1p or Tris1Del1p vs. Dis1Del1p ($P = 0.014$, $P < 0.001$, or $P = 0.003$). Infants diagnosed clinically: Dis1Norm1p or Tris1Norm1p vs. Dis1Del1p ($P = 0.079$ or $P < 0.001$). Children diagnosed clinically: Dis1Norm1p or Tris1Norm1p vs. Dis1Del1p ($P < 0.006$ or $P < 0.006$).

showed that of 94 with 3 or 4 normal chromosome 1 s, and both had many double minutes.

Three Biological Types of Neuroblastomas Defined by the Number of Chromosome 1 and *MYCN* Status, and Survivals and Stage of the Disease in Patients With Each Type of the Tumors

The OS was excellent in infants found by MS, dismal in children diagnosed clinically, and intermediate in infants diagnosed clinically (Table I). Because there was no significant difference in OS between patients with Tris1Norm1p tumors and those with Tris1Del1p tumors in all three clinical groups (infants found by MS, infants diagnosed clinically, and children diagnosed clinically), OS of Tis1Norm1p patients was combined with that of Tris1Del1p patients. The OS of patients with Dis1Del1p tumors was worse than that of patients with Dis1Norm1p tumors in all three clinical groups (Table I). The OS was better for the 12 patients with Dis1Del1p tumors with no *MYCN* amplification than for the four patients with Dis1Del1p tumors with *MYCN* amplification in infants found by MS ($P < 0.001$). In contrast, the OS did not differ between the patients with Dis1Del1p tumors with no *MYCN* amplification and those with Dis1Del1p tumors with *MYCN* amplification in infants or children diagnosed clinically. In addition, there was no significant difference in OS between the patients with Dis1Norm1p tumors and those with Dis1Del1p tumors with no *MYCN* amplification in infants found by MS or infants diagnosed clinically. Children diagnosed clinically with Dis1Norm1p tumors tended to show the better OS than those with Dis1Del1p tumors with no *MYCN* amplification ($P = 0.078$).

Thus, the 453 tumors were classified into three biological types: type 1, 313 tumors with Tris1Norm/Del1p with no *MYCN* amplification; type 2, 89 tumors with Dis1Norm/Del1p with no *MYCN* amplification; type 3, 46 tumors with Dis1Del1p with *MYCN* amplification (Table II). Of five patients with Tris1Norm/Del1p tumors with *MYCN* amplification, an infant diagnosed clinically with five copies of *MYCN* at stage 2 and a child diagnosed clinically with 10 copies at stage 3 were alive, and the other three children diagnosed clinically with more than 10 copies at stage 4 died of the disease. The five tumors with Tris1 with *MYCN* amplification were excluded in the subsequent analysis because of the rare incidence of the combination.

Type 1 tumors in infants found by MS or diagnosed clinically had earlier stages of the disease than type 1 tumors in children diagnosed clinically ($P < 0.0001$ and $P = 0.0007$) (Table II). Type 2 tumors in infants found by MS tended to have earlier stages than type 2 tumors in infants diagnosed clinically ($P = 0.06$) and showed earlier stages than type 2 tumors in children diagnosed clinically ($P < 0.0001$). There was no significant difference in the stage distribution of type 3 tumors between any 2 of the three clinical groups (infants found by MS, infants diagnosed clinically and children diagnosed clinically).

The OS was better for infants with type 1 tumors found by MS ($P < 0.001$) or for infants with type 1 tumors diagnosed clinically ($P = 0.005$) than for children with type 1 tumors diagnosed clinically (Fig. 2). There was no significant difference in the OS between type 1 infants detected by MS and type 1 infants diagnosed clinically. The OS was better for infants with type 2 tumors found by MS than for infants with type 2 tumors diagnosed

TABLE II. Three Biological Types of Neuroblastoma Classified by the Number of Chromosome 1 and *MYCN* Status in Three Groups of Patients Classified by the Age of Patients and the Method of Tumor Detection

Group of patients	Number of patients	Stage of disease					Overall survival at 6 years	
		1	2	4S	3	4	%	Standard error
Infants found by mass-screening								
Type 1 (Tris1 with normal *MYCN*) tumor	253	111	66	21	39	16	99.6	0.4
Type 2 (Dis1 with normal *MYCN*) tumor	30	11	7	9	1	2	100	
Type 3 (Dis1 with amplified *MYCN*) tumor	4	0	0	0	0	4	0	
Total	287	122	73	30	40	22	98.2	0.8
Infants diagnosed clinically (<12 months)								
Type 1 (Tris1 with normal *MYCN*) tumor	34	15	5	7	6	1	97.1	2.9
Type 2 (Dis1 with normal *MYCN*) tumor	12	1	2	4	2	3	72.9	13.5
Type 3 (Dis1 with amplified *MYCN*) tumor	4	0	0	2	1	1	25.0	21.7
Total	50	16	7	13	9	5	85.3	5.1
Children diagnosed clinically (≥12 months)								
Type 1 (Tris1 with normal *MYCN*) tumor	26	5	6	0	4	11	68.6	9.2
Type 2 (Dis1 with normal *MYCN*) tumor	47	3	4	0	6	34	53.5	7.4
Type 3 (Dis1 with amplified *MYCN*) tumor	38	0	2	0	7	29	35.6	8.0
Total	111	8	12	0	17	74	50.9	4.9

Tris1, trisomy 1; Dis1, disomy 1. See the text for more detailed definition.